Available online at www.sciencedirect.com
SCIENCE DIRECT®
Precambrian Research 141 (2005) 83–105
Precambrian Research
www.elsevier.com/locate/precamres

The Gurupi Belt, northern Brazil: Lithostratigraphy, geochronology, and geodynamic evolution

Evandro L. Klein [a,*], Candido A.V. Moura [b], Robert S. Krymsky [b,1], William L. Griffin [c,d]

[a] *CPRM/Geological Survey of Brazil, Av. Dr. Freitas, 3645, Belém-PA CEP 66095-110, Brazil*
[b] *Laboratório de Geologia Isotópica/Pará-Iso, Universidade Federal do Pará, Centro de Geociências, CP 1611, Belém-PA CEP 66075-900, Brazil*
[c] *ARC National Key Centre for Geochemical Evolution and Metallogeny of Continents, Department of Earth and Planetary Sciences, Macquarie University, NSW 2109, Australia*
[d] *CSIRO Exploration and Mining, North Ryde, NSW 2113, Australia*

Received 11 December 2004; received in revised form 20 July 2005; accepted 19 August 2005

Abstract

The Gurupi Belt is located in northern Brazil on the southern margin of the São Luís Craton, which is dominated by juvenile calc-alkaline rocks formed in intra-oceanic island arcs between 2240 and 2150 Ma. The Gurupi Belt consists of: (i) small lenses of an Archean metatonalite of 2594 Ma; (ii) calc-alkaline/TTG tonalites and gneisses of 2147–2168 Ma and juvenile Nd isotope signature, formed in intra-oceanic arc setting; (iii) an I-type monzogranite that intruded by ca. 2159 Ma, formed by the reworking of the oceanic arcs; (iv) a metavolcano–sedimentary succession with calc-alkaline volcanic rocks of 2148–2160 Ma and juvenile Nd isotope signature formed in arc systems; (v) several peraluminous, muscovite-bearing, collision-type granites of 2070–2100 Ma with Nd isotopes indicating variable reworking (partial melting and/or erosion) of Paleoproterozoic and Archean crust; (vi) a sub-greenschist- to greenschist-facies supracrustal sequence of unknown age (tentatively considered to be older than 2159 Ma); (vii) an amphibolite-facies metasedimentary sequence in which the youngest detrital zircon has age of 1100 Ma, and Nd isotopes and sedimentological evidence indicating Archean, Paleoproterozoic, Mesoproterozoic, and Neoproterozoic sources; (viii) a deformed (gneissic) nepheline syenite of 732 Ma formed by mixing of mantle and crustal sources; (ix) a peraluminous, muscovite-bearing post-tectonic granite of 549 Ma. Combined geological and geochronological information indicate that the Paleoproterozoic rocks are part of a Trans-Amazonian/Eburnean orogen initiated by an accretionary phase (2240–2150 Ma), better represented in the adjacent São Luís Craton, and terminated by a collisional event (2100–2080 Ma) that amalgamated juvenile and reworked Paleoproterozoic terrains and an Archean terrain existing to the south. This landmass amalgamated in the Paleoproterozoic broke up before 732 Ma, forming a rift, as suggested by the emplacement of the nepheline syenite pluton. The rift received detritus coming from Archean, Paleoproterozoic, Mesoproterozoic, and Neoproterozoic sources. We infer that the rift evolved to an oceanic basin and that the closure of this basin occurred at the end of the Neoproterozoic (580–550 Ma), as part of the Brasiliano/Pan-African cycle of orogenies.

Keywords: Zircon geochronology; Nd isotopes; Crustal evolution; Gurupi Belt; Paleoproterozoic; Neoproterozoic

1. Introduction

Early geochronological studies, using the conventional Rb–Sr and mineral K–Ar systems (Hurley et al., 1967, 1968; Almeida et al., 1968; Cordani et al.,

* Corresponding author. Tel.: +55 91 3276 8577; fax: +55 91 3276 4020.
E-mail address: eklein@be.cprm.gov.br (E.L. Klein).
[1] Present address: All-Russian Geological Research Institute (VSEGEI), Sredny Prospect, 74, Saint Petersburg 199106, Russia.

0301-9268/$ – see front matter © 2005 Elsevier B.V. All rights reserved.
doi:10.1016/j.precamres.2005.08.003

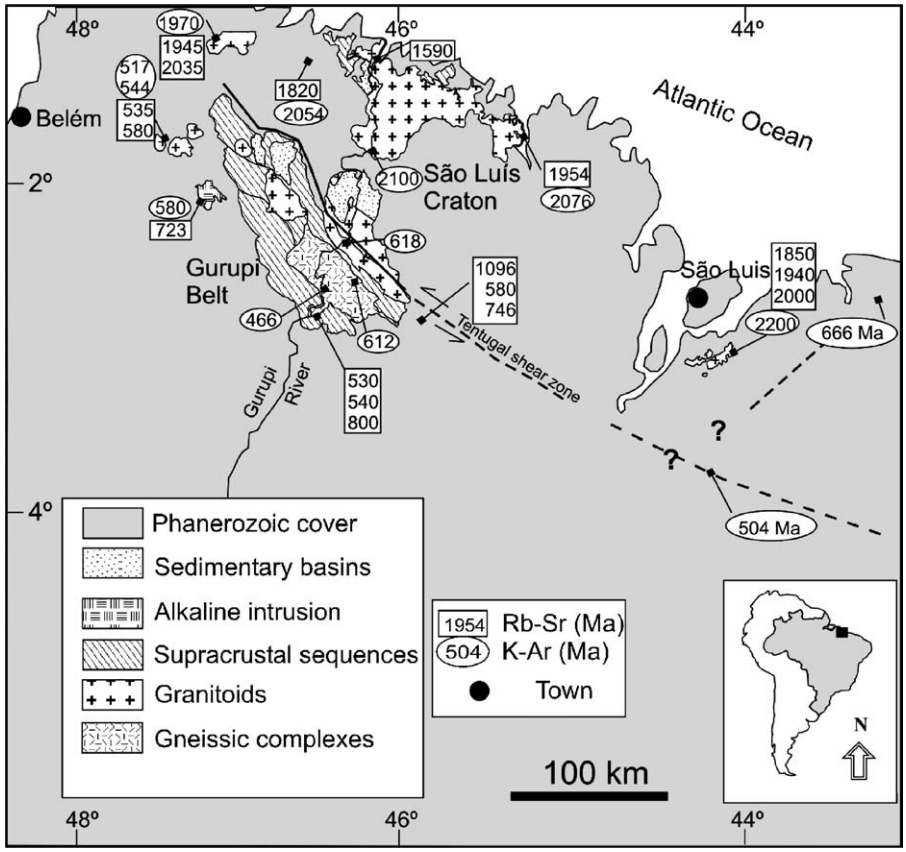

Fig. 1. Simplified geological map of the Gurupi region. The location of the main available Rb–Sr and K–Ar ages that defined the two geochronological domains (Gurupi Belt and São Luís Craton) is also shown. Sources for the data are in Table 1.

1968, 1974; Almaraz and Cordani, 1969), defined two geochronological provinces in the NE part of Pará state and the NW part of Maranhão state, northern Brazil. Those studies showed that the rocks cropping out toward the Atlantic coastline have a Paleoproterozoic signature, whereas the rocks cropping out toward the inner parts of the continent have been affected by Neoproterozoic events (Fig. 1). These Paleoproterozoic and Neoproterozoic provinces have then been named São Luís Craton and Gurupi Belt, respectively (Almeida et al., 1976), and the boundary between these two provinces has been defined as being the Tentugal shear zone (Hasui et al., 1984).

Several regional-scale mapping programs have been carried out over 20 years in this region, each accompanied by lithostratigraphic proposals and geotectonic models (Costa et al., 1977; Abreu et al., 1980; Hasui et al., 1984; Pastana, 1995; Costa, 2000; Almeida, 2000), always based on the available Rb–Sr and K–Ar data. Discussions concerning the concept, geographic distribution, inferred age, and tectonic setting of some lithostratigraphic units, in addition to geotectonic models, with propositions favoring either a mono- or poly-phase evolution for the belt, fomented the debate throughout the past two decades. Correlations between the São Luís and West African cratons, and between the Gurupi Belt and the Pan-African belts that border the West African Craton, have been made as well (Torquato and Cordani, 1981; Lesquer et al., 1984; Abreu and Lesquer, 1985).

Recent studies, using more robust geochronological systems (single zircon Pb evaporation and whole rock Sm–Nd), along with new field and petrographic information, have brought out interesting constraints with implications for the lithostratigraphy and developing geotectonic models. Palheta (2001) has demonstrated that several granitoid plutons, previously grouped as a Neoproterozoic collisional suite (Costa, 2000), actually belong to at least three different generations, showing Paleoproterozoic and Neoproterozoic crystallization ages, and Paleoproterozoic to Archean model ages. Klein and Moura (2001) have defined Paleoproterozoic ages (2148–2160 Ma) for metavolcanic rocks from the major metavolcano–sedimentary sequence of the belt, and Klein and Moura (2003) have determined a Pale-

oproterozoic minimum age (2135 Ma) for amphibolite-facies gneisses that have previously been considered as having Archean ages (Pastana, 1995) by correlation with compositionally similar rocks of the Amazonian Craton. Therefore, these studies anticipate a more complex evolutionary history for the Gurupi Belt.

Despite these advances, the age of some units is still not constrained by robust methods, and field relationships between different units are only rarely observed, hindering a better establishment of the relative stratigraphy; this makes geochronology an indispensable tool. Furthermore, the relative contributions of crustal and mantle sources in the genesis of the various rock units is known only for a few granite bodies, hindering the discussion of the crustal evolution of the belt. For instance, were all the igneous rocks of the Gurupi Belt produced by reworking of a pre-existing crust, as suggested from the Sm–Nd data presented by Palheta (2001), or are juvenile components also present? What is the age of the Tentugal shear zone? Does the Tentugal shear zone represent a suture between the Gurupi Belt and the São Luís Craton? What is the meaning of the Neoproterozoic Rb–Sr and K–Ar ages? What was the paleogeography of the belt; that is, in what kind of tectonic setting have the distinct units formed? Since most of the rocks in the Gurupi Belt are Paleoproterozoic, what were the relationships of these rocks with the Paleoproterozoic and dominantly juvenile (Klein et al., 2005) rocks of the São Luís Craton?

It is the intention of this paper to address some of these questions. We present a review of the main geological attributes of the Gurupi Belt, including lithology, metamorphism, structure, limits, previous geochronology, and geotectonic models. We provide new field information, geochronological data on zircon (Pb evaporation, U–Pb), and Sm–Nd isotope compositions of metavolcanic, metaplutonic, and metasedimentary rocks. As such, all igneous and metaigneous, and most of the metasedimentary units of the belt have now at least one geochronological age based on zircon, which better constrains the regional lithostratigraphy. Furthermore, accretion and/or reworking and possible geological settings are assessed by a combination of zircon geochronology, Sm–Nd isotopes, and rock association. Unresolved problems that need further investigation are highlighted as well.

2. Geological overview

2.1. Geographical extent and limits

The Gurupi Belt trends NNW/SSE; its present-day cropping area is about 160 km long and up to 50 km wide. The boundary between the Gurupi Belt and the São Luís Craton has usually been considered as being the Tentugal shear zone (Fig. 1), which is also interpreted as the suture between these two terranes (Hasui et al., 1984; Abreu and Lesquer, 1985). However, most of the rock units in the belt crop out as discontinuous erosive and tectonic windows within Phanerozoic sedimentary basins (Fig. 1), hindering a clear definition of the other limits of the belt. Some attempts have been made to assess these limits by the investigation of the basement of the Phanerozoic basins using geophysical and subsurface information (drill cores that attained the basement units), in addition to the available Rb–Sr and K–Ar evidence (Brito Neves et al., 1984; Cordani et al., 1984; Cunha, 1986; Nunes, 1993). These studies indicate that the concealed portion of the Gurupi Belt extends for about 60–80 km to the south and about 500 km to the east–southeast (Figs. 1 and 2). The southernmost limit of the belt appears to be the so-called Parnaíba block, which was described by Cunha (1986) as being a supposed cratonic nucleus that would have distinct age and structural trends in relation to the surrounding terranes. The easternmost limit of the São Luís Craton might have direct links with the Médio Coreaú domain of the Borborema Province (Fig. 2), which is composed of Paleoproterozoic basement rocks, mainly gneisses and migmatites, that have been reworked in the Neoproterozoic (e.g., Brito Neves et al., 2000). To the west, the limits are still obscure (Fig. 2). An interesting feature also shown by Fig. 2 is the sequence labeled supracrustal rocks that has the same structural trend showed by the exposed portion of the Gurupi Belt. The relationship of this sequence with the rocks of the Gurupi Belt is not clear. Another important feature is the Transbrasiliano Lineament, a major tectonic zone that has been active in the Neoproterozoic.

2.2. Structure

Most of the sequences of the Gurupi Belt form elongated bodies that are parallel to the longest dimension of the belt, i.e., NW–SE. Planar structures such as incipient cleavage, penetrative schistosity, S–C fabric, mylonitic foliation, and gneissic banding are recognized throughout the belt. The angular relationships between the planar and linear features broadly form two domains in a regional scale. Low- to moderate-angle planar structures with associated down-dip or oblique lineations are mostly confined to the northwestern portion of the belt, and dip generally to south–southwest. Steeply dipping planar structures and associated low-angle lineations concentrate in the central and southeastern portions (Fig. 3). These relationships have usually been

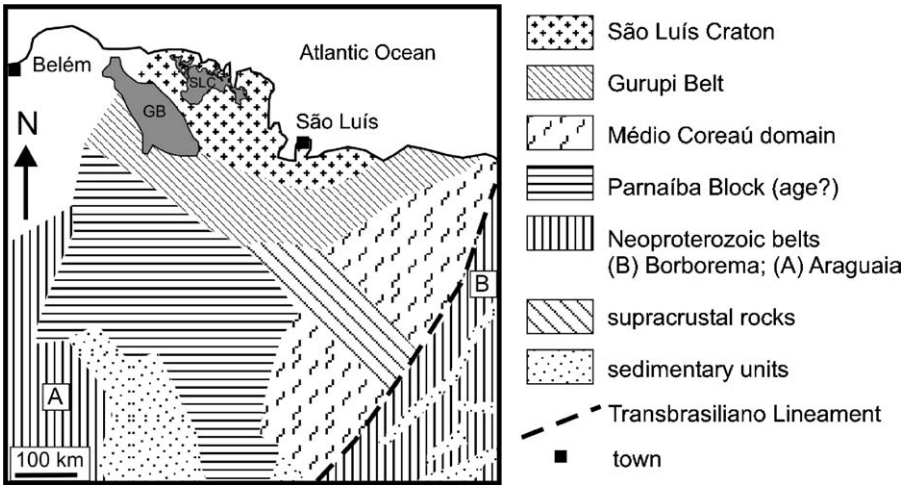

Fig. 2. Sketch map showing the position of the present-day cropping area of the Gurupi Belt (GB) and São Luís Craton (SLC) in relation to the interpreted map of the basement of the Phanerozoic cover. The map was constructed using geophysical and structural information, in addition to petrographic and geochronological information obtained from drill cores that attained the basement rocks of the Phanerozoic cover (redrawn from Brito Neves et al., 1984; Cunha, 1986; Nunes, 1993—see text for additional explanation).

interpreted in terms of oblique collision of the Gurupi Belt against the São Luís Craton, accompanied and/or followed by sinistral strike–slip (escape) tectonics (Costa et al., 1988; Pastana, 1995; Costa, 2000).

The Tentugal shear zone represents most of the strike–slip domain that is located in the boundary zone between the São Luís Craton and the Gurupi Belt (Hasui et al., 1984; Abreu and Lesquer, 1985). In a recent study, Ribeiro (2002) addressed in more detail the architecture, geometry, kinematics, and evolution of this major structure, using structural mapping and high-resolution geophysical data. This segment records multiple deformation episodes that resulted in a complex finite structural framework, and Ribeiro (2002) stated that the methodologies employed have not allowed either the reconstruction of the timing of the deformation events or the correlation of all observed structures with the deformation events that produced them. In other words, it is still uncertain if the observed structural framework within the Tentugal shear zone records a single and progressive major deformation event, or if it was produced by two or more distinct events separated in the geological time. Notwithstanding, Ribeiro (2002) concluded that the strike–slip system is a segment of a shear belt formed in response to an oblique collision with a strong transcurrent component.

2.3. *Lithostratigraphy, metamorphism, and previous geochronology*

The Gurupi Belt is a plutonic–metamorphic belt composed of metasedimentary and metavolcano–sedimentary sequences, gneisses, and several generations of granitoids and alkaline rocks (Fig. 3). Available geochronological data for these units are displayed in Table 1.

Orthogneisses are grouped in the Itapeva Complex (Klein, 2004), and consist of foliated to banded and locally folded rocks that underwent amphibolite-facies metamorphism and local migmatization. Compositionally, the orthogneisses are tonalites and subordinate granodiorites. They are mainly biotite- and subordinately amphibole-bearing rocks, while muscovite indicates retrograde effects. Geochemical information is not available, but these rocks probably belong to a calc-alkaline and/or TTG association. The gneisses exhibit tectonic contacts with the Chega Tudo and Marajupema supracrustal formations (Fig. 3), and with the Maria Suprema Granite (Fig. 4). The metamorphic banding consistently strikes to N40°–50°W, and dips >75° to the southwest. Mineral lineations have gentle to steep plunges, indicating the predominance of oblique transcurrence. Conventional Rb–Sr ages (Hurley et al., 1967, 1968) are in the 530–800 Ma range, and an age of 2135 ± 4 Ma has been obtained by Klein and Moura (2003) in a tonalitic gneiss, using the zircon Pb evaporation technique; this is interpreted as a minimum age for the emplacement of the igneous protolith of the gneiss. In a granitic vein, folded coaxially to the gneissic banding, Klein and Moura (2003) found zircons of Paleoproterozoic and Archean ages. The Archean ages are 2580 and 2607 Ma, whereas the Paleoproterozoic zircons have ages in the 2100 ± 20 Ma range, and very low Th/U ratios (0.03). These low ratios may indicate a metamorphic

Table 1
Summary of the main previous geochronological data of rocks from the Gurupi Belt and adjoining São Luís Craton

Unit	Rock types	Zircon[a] (Ma)	Rb–Sr (Ma)	K–Ar (Ma)	Sm–Nd T_{DM} (Ga)/ε_{Nd_T}	References
São Luís Craton						
Tromaí Intrusive Suite	Tonalite, granodiorite	2147–2168	(1590) 1954–2100	2076	2.22–2.26/(1.9, 2.6)	(1, 2) (3,4,5) (4) (2)
Rosário Intrusive Suite	Tonalite, granodiorite	2075–2146	1850–2000	2200	2.1/(2.5)	(6) (3) (7) (8)
Tracuateua Intrusive Suite	Granite	2086–2091	1945–2047	1906–2056	2.3–2.5/(−1.3, 1.5)	(9) (3, 10) (7, 10) (9)
Aurizona Group	Volcano–sedimentary	2240 ± 5	na	na	2.21–2.48/(0.8, 3.5)	(1) (2)
Basement of Phanerozoic Basin	Metasedimentary	na	1820	2054	na	(11) (5)
Gurupi Belt						
Itapeva Complex	Tonalite gneiss	2135 ± 4	530–800	466–612	na	(12) (3) (5)
Chega Tudo Formation	Felsic metavolcanic	2148–2160	na	na	na	(1)
Tromaí Intrusive Suite	Tonalite	2148 ± 4	na	618	na	(1) (5)
Cantão Granite	Monzogranite	2159 ± 13	na	na	2.21–2.48/(2.7, −0.9)	(9) (9)
Japiim Granite	Monzogranite	2084 ± 5	na	na	2.22–3.23/(1.9, −3.4)	(9) (9)
Jonasa Granite	Granodiorite	2061 ± 8	2018 ± 61 (525 ± 20[b])	na	2.09–2.40/(3.2, −1.1)	(9) (12) (9)
Ourém Granite	Monzogranite	2011 ± 6	na	na	na	(9)
Maria Suprema Granite	Syenogranite	na	(1710 ± 32[b])	na	na	(1)
Boca Nova Nepheline Syenite	Nepheline-syenite	na	723 ± 30	580 ± 10	na	(13) (14)
Ney Peixoto Granite	Syenogranite	549 ± 4	535–580	517–544	1.70/(−8)	(9) (3, 13) (3, 7, 13) (9)
Basement of Phanerozoic Basin	Granitoids	na	na	666	na	(7)
Basement of Phanerozoic Basin	Metasedimentary	na	580–1096	504	na	(11) (7)

Key to references: (1) Klein and Moura (2001); (2) Klein et al. (2005); (3) Hurley et al. (1967, 1968); (4) Costa et al. (1977); (5) Sadowski (2000); (6) Gorayeb et al. (1999); (7) Almeida et al. (1968); (8) Sato (1998); (9) Palheta (2001); (10) Wanderley Filho (1980); (11) Cordani et al. (1984); (12) Klein and Moura (2003); (13) Villas (1982); (14) Jorge-João (1980). na: not available.

[a] Pb evaporation ages.

[b] Internal isochrone (minerals + whole rock).

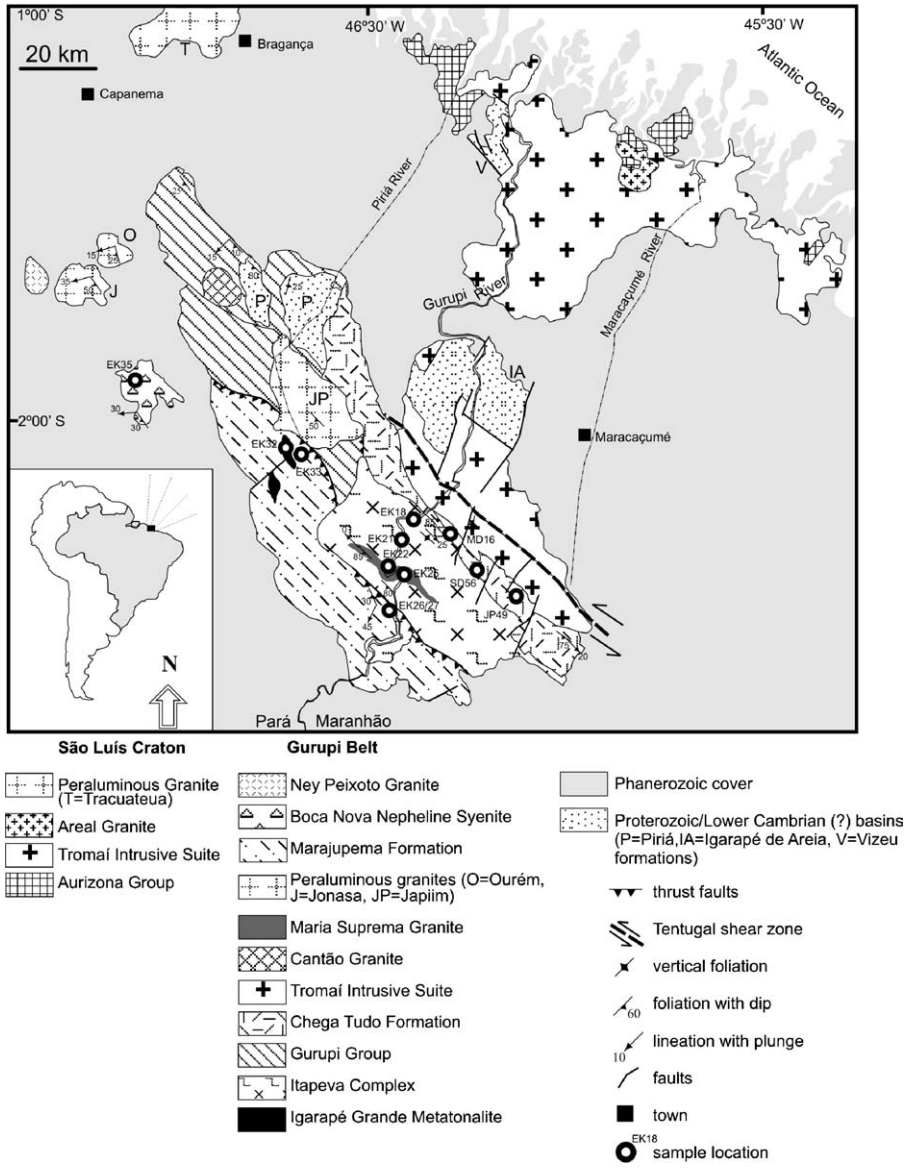

Fig. 3. Geological map of the Gurupi Belt and São Luís Craton, with the location of the samples analyzed in this study.

environment or migmatization/partial melting in a Th-poor lower crust (Kröner et al., 1994; Bartlett et al., 1998; Möller et al., 2003). Small lenses of granoblastic metatonalite to gneiss have also been included in this complex by Almeida (2000). However, these lenses are grouped here in a distinct unit, named the Igarapé Grande Metatonalite (Fig. 3).

Large wedges of amphibole- and/or biotite-bearing tonalites and granodiorites belonging to the Tromaí Intrusive Suite, which is the largest unit of the São Luís Craton, have been tectonically reworked in the boundary zone between the craton and the Gurupi Belt, and are included in the framework of the belt (Fig. 3). Structurally, therefore, these granitoids show variable intensities of deformation, from a weak foliation to ultramylonite fabric, depending on the proximity of shear zones. The foliation is parallel to the regional NW–SE trend of the Tentugal shear zone, and stretching lineations plunge at very low angles, generally to the southwest. Granitoids of the suite have zircon Pb evaporation ages between 2168 and 2147 Ma (Klein and Moura, 2001, 2003), Sm–Nd model ages (T_{DM}) of 2.22–2.26 Ga with ε_{Nd} values of +1.9 to +2.6, and show calc-alkaline to TTG chemical signatures. These granitoids are inter-

Fig. 4. Outcrop showing a tonalite gneiss of the Itapeva Complex intruded by leucogranite sheets belonging to the Maria Suprema unit (outlined by the dashed lines). View toward northwest.

preted to have formed from juvenile protoliths in intra-oceanic arc systems (Klein et al., 2005).

The Cantão Granite is a rounded body (Fig. 3) of weakly deformed biotite-bearing monzogranite showing enclaves of metavolcanic and metasedimentary rocks, a feature that has been used as evidence of intrusion of this pluton in the enclosing Gurupi Group (Costa, 2000; Palheta, 2001). Palheta (2001) obtained a zircon age of 2159 ± 13 Ma and Sm–Nd model ages between 2.21 and 2.48 Ga, with positive to slightly negative ε_{Nd} values (Table 1).

Pastana (1995) described the Maria Suprema Granite as corresponding to a single body (Fig. 3) of mylonitic, muscovite-, and biotite-bearing leucogranite. In the field, this granite occurs in discontinuous meter- to decameter-thick layers or sheets that crop out in structural conformity with the gneisses of the Itapeva Complex (Fig. 4). The rocks have a strongly developed foliation with structural features recording the imprint of a strike–slip regime. The structural and compositional evidence suggests that the Maria Suprema Granite represents a peraluminous syntectonic intrusion. An internal isochrone (muscovite + K-feldspar + whole rock) gave an age of 1710 ± 32 Ma (Table 1). This age was interpreted as the product of partial resetting of the Rb–Sr system, without geological relevance, indicating only a minimum age for the emplacement of the granite (Klein and Moura, 2001).

Three other bodies of biotite- and muscovite-bearing peraluminous granites (Japiim, Jonasa, and Ourém) exhibit rounded to irregular shapes (Fig. 3). The Jonasa and Ourém plutons are mostly covered by the Phanerozoic sedimentary rocks, hindering the establishment of the relationships with their host rocks. For the Japiim pluton, Costa (2000) described the presence of granite dykes cutting across the surrounding supracrustal rocks, indicating intrusional relationships between the granite and the Gurupi Group. These peraluminous granites display a variety of petrographic composition, from true granite to subordinate granodiorite, and are variably foliated. The foliation is concordant with the regional NW–SE trend of the Gurupi Belt, and stretching lineations plunge with low angles (15–35°) to the southwest in the Jonasa and Ourém plutons, and with moderate to high angles (>60°) in the Japiim pluton (Costa, 2000; Palheta, 2001). Palheta (2001) reported Pb evaporation zircon ages of 2061 ± 8 for the Jonasa Granite, along with inherited zircons with ages between 2325 and 2446 Ma; Sm–Nd T_{DM} model ages lie between 2.09 and 2.40 Ga, with slightly positive to negative ε_{Nd} values (Table 1). Klein and Moura (2003) determined an Rb–Sr isochrone age of 2018 ± 61 Ma for this granite, with an initial $^{87}Sr/^{86}Sr$ of 0.7034; the age is in agreement with the zircon age. Klein and Moura (2003) also determined an internal isochrone (whole rock + feldspar + muscovite + biotite) of 525 ± 20 Ma. This isochrone indicates that while the Rb–Sr system remained closed at the whole rock scale, it records the overprint of a Neoproterozoic event. The petrographic, geochronological, and isotopic information suggest that both Paleoproterozoic and Archean crustal protoliths (sedimentary- and igneous-derived) are the probable magma sources for the Jonasa Granite. Palheta (2001) also determined an age of 2084 ± 5 Ma for the Japiim Granite, with one inherited crystal with an age of 2351 Ma, in addition to T_{DM} model ages of 2.22 and 3.23 Ga, and ε_{Nd} values of +1.9 and −3.4, respectively, which imply a contribution of Archean protoliths to the source magmas.

All the supracrustal sequences of the Gurupi Belt have previously been grouped in a single unit termed the Gurupi Group (Pastana, 1995; Costa, 2000). Costa (2000), working in the northwestern portion of the Gurupi Belt, described the Gurupi Group as composed almost exclusively of metasedimentary rocks, and interpreted the sequence as deposited on a passive continental margin. Part of this sequence, however, was revealed to be comprised of metavolcano–sedimentary rocks (Ribeiro, 2002; Klein, 2004), and is considered as an independent unit (Fig. 3), defined as the Chega Tudo Formation (Klein, 2004), not belonging to the Gurupi Group. The Chega Tudo Formation consists of metavolcanic rocks with predominance of dacite and rhyodacite, and lesser proportions of andesite, basalt, and mafic to ultramafic schists; volcaniclastic rocks; sedimentary-derived quartz-, mica-, and graphite-bearing schists (pelites). Metamorphosed and variably deformed diorite, gabbro, and wherlite have also been identified in underground workings, occurring as lenses intercalated within the volcano–sedimentary pile (Ribeiro, 2002). The rocks

are highly strained, since they are located within the most active domain of the Tentugal shear zone. The NW–SE-trending foliation strikes at very steep angles, mostly to the southwest, and stretching lineations are subhorizontal. Scarce whole rock geochemical data (Dias, 1983) indicate that the felsic to intermediate volcanic rocks have calc-alkaline signatures, whereas the mafic volcanics show ambiguous characteristics between island arc tholeiites and calc-alkaline basalts, and subordinate within-plate basalts. Felsic metavolcanic rocks of this unit have been dated at 2148–2160 Ma by the zircon evaporation technique (Klein and Moura, 2001).

The remaining Gurupi Group comprises a lower unit composed of sub-greenschist-facies rocks, mainly pelites, and an upper unit composed of greenschist-facies (biotite isograd) rocks, mainly quartz- and mica-rich schists (Costa, 2000). Limited structural information (Fig. 3) shows dominantly low-angle structures. This sequence lacks geochronological information on zircon, and is tentatively considered as being older than 2159 Ma, which is the age of the Cantão Granite that supposedly intruded the rocks of the Gurupi Group (Costa, 2000; Palheta, 2001).

The Marajupema Formation (Klein, 2004) is a siliciclastic succession composed of coarse-grained and banded feldspathic schists, with or without garnet and chloritoid; feldspathic quartzites with variables amounts of cordierite, garnet, muscovite, biotite, and plagioclase; and of muscovite-bearing orthoquartzites. The mineral paragenesis is compatible with amphibolite-facies conditions. Field evidence shows structures with moderate (45–65°) dips and plunges, and the sequence is interpreted to have overthrusted the Itapeva Complex and the Gurupi Group (Fig. 3). There are no previous geochronological data for this unit.

The nepheline-syenite gneiss of Boca Nova is an isolated body that is also mostly covered by Phanerozoic sedimentary basins (Fig. 3). It is composed of nepheline, albite, perthite, plagioclase, and biotite, in addition to accessory phases such as pyrochlore, apatite, zircon, carbonate, sodalite, cancrinite, white mica, and pyrite (Villas, 1982). The rock is compositionally homogeneous and has been deformed and metamorphosed under amphibolite-facies conditions (Lowell and Villas, 1983), which produced a gneissic fabric and local migmatization. This NW–SE-trending gneissic banding dips at low angles to the west–southwest. Whole rock geochemical data presented by Lowell and Villas (1983) showed that the nepheline syenite is a peralkaline to weakly metaluminous rock, having high Rb, Sr, Nb, Ba, and Zr contents. A Rb–Sr isochrone age of 723 ± 30 Ma, with initial $^{87}Sr/^{86}Sr$ of 0.7034, has been reported by Villas (1982), and Jorge-João (1980) determined a K–Ar age of 580 ± 10 Ma on biotite. Based on the geochemical data and the low $^{87}Sr/^{86}Sr$ initial ratio of 0.7034, Lowell and Villas (1983) interpreted the nepheline syenite as being derived from the fractional crystallization of mantle-derived trachyte magma. There is no unequivocal interpretation regarding the timing of emplacement of this unit and the meaning of the geochronological information. Lowell and Villas (1983) regarded the Rb–Sr age as geologically meaningless, representing the partial resetting of the isotopic system; therefore, it could represent neither the emplacement age nor the metamorphic age, which would be represented by the K–Ar age.

The Ney Peixoto Granite is a small rounded body of granite also covered by Phanerozoic sedimentary rocks. It is biotite- and muscovite-bearing granite that shows an incipient NW–SE-trending foliation dipping at high angles to the southwest. This granite is petrographically very similar to the Paleoproterozoic peraluminous granitoids. However, it shows a zircon age of 549 ± 4 Ma and a Sm–Nd model age of 1.70 Ga, with a ε_{Nd} value of −8 (Palheta, 2001). It also shows a Rb–Sr isochrone age of 580 ± 58 Ma, and initial $^{87}Sr/^{86}Sr$ of 0.704 (Villas, 1982). A peraluminous chemical and mineralogical signature, with a moderately fractionated REE pattern and pronounced Eu anomaly, was described by Villas (2001). The chemical and isotopic information indicate mixed sedimentary and igneous crustal sources (Villas, 2001) for this granite.

Piriá is a small sedimentary basin that unconformably overlies the supracrustal sequences of the Gurupi Belt (Fig. 3), having distinct lithologic, metamorphic, and structural aspects (Abreu et al., 1980). It is dominated by arkoses, pelites, and conglomerates deposited in shallow lake or marine waters (Truckenbrodt et al., 2003). The rocks exhibit incipient foliation with variable orientations, in general parallel to the sedimentary bedding, and locally underwent anchimetamorphism (Costa, 2000). There are no geochronological data available for this sedimentary formation. However, the upper limit of its depositional age is probably about 550 Ma by correlation with the nearby and similar Igarapé de Areia Formation of the São Luís Craton that contains detrital zircons with this age (Pinheiro et al., 2003).

2.4. The São Luís Craton

Due to its bearing in the regional geodynamic evolution, a brief review of the São Luís Craton is presented here. For more details, the reader is referred to Klein and Moura (2001, 2003), Klein et al. (2005), and their references. The craton is composed of a few suites of grani-

toids, and of a metavolcano–sedimentary sequence, both being covered by younger sedimentary basins (Fig. 3).

The metavolcano–sedimentary succession (Aurizona Group) consists of schists of variable compositions, metavolcanic and metapyroclastic rocks, and of subordinate quartzite, metachert, and metamafic–ultramafic rocks. The metamorphic conditions are predominantly of the greenschist facies, but attained locally the lower amphibolite facies. Only one sample of this sequence has been dated so far, yielding an age of 2240 ± 5 Ma (Pb–Pb zircon), with Sm–Nd T_{DM} model age of 2.21–2.48 Ga, and $\varepsilon_{Nd}(t)$ values of +0.8 to +3.5.

The Tromaí Intrusive Suite has already been described in Section 2.3. In the cratonic area, however, the rocks do not show the effects of deformation as they do in the Gurupi Belt, except along narrow shear zones. Instead, the suite forms batholiths of porphyritic to equigranular and massive to weakly foliated tonalite, trondhjemite, granodiorite, and minor monzogranite. Areal is another unit of calc-alkaline rocks, composed of K_2O-enriched true granites of 2150 Ma (Pb–Pb zircon) with Sm–Nd T_{DM} model age of 2.23–2.26 Ga, and $\varepsilon_{Nd}(t)$ values of +1.9 to +2.3, that is, broadly the same Sm–Nd patterns exhibited by the Tromaí suite. The Areal Granite is interpreted to have formed by the reworking of the island arcs in which the Tromaí and Aurizona units formed.

The Tracuateua Intrusive Suite consists of S-type, strongly peraluminous two-mica granites, derived from the partial melting of crustal rocks, having zircon Pb evaporation ages of 2086–2091 Ma, and Sm–Nd model ages (T_{DM}) varying between 2.31 and 2.50 Ga, with $\varepsilon_{Nd}(t)$ values ranging from −1.3 to +1.1.

3. Sampling and analytical procedures

Sampling sites are showed in Fig. 3. Zircons were dated by the single zircon Pb evaporation, U–Pb isotopic dilution (ID-TIMS), and U–Pb laser ablation (LAM-ICP-MS) methods, and whole rock samples were analyzed for their Sm–Nd isotope compositions. The Pb evaporation, ID-TIMS, and Sm–Nd analyses were conduced at the Laboratório de Geologia Isotópica (Pará-Iso) of the Universidade Federal do Pará, Belém, Brazil, using a Finnigan Mat 262 mass spectrometer, whereas the LAM-ICP-MS analyses were performed at the Macquarie University, Sidney, Australia. Zircon crystals were separated by handpicking of selected grains under binocular microscope, from concentrates obtained after crushing and sieving the samples, and magnetic and heavy liquids separation.

For the Pb evaporation method (Kober, 1986, 1987), the double filament array was used and data were acquired in the dynamic mode using the ion-counting system of the instrument. For each step of evaporation, a step age is calculated from the average of the $^{207}Pb/^{206}Pb$ ratios. When different steps yield similar ages, all are included in the calculation of the crystal age. If distinct crystals furnish similar mean ages, then a mean age is calculated for the sample. Crystals or steps showing lower ages probably reflect Pb loss after crystallization (e.g., Vanderhaeghe et al., 1998) and are not included in sample age calculation. Common Pb corrections were made according to Stacey and Kramers (1975) and only blocks with $^{206}Pb/^{204}Pb$ ratios higher than 2500 were used for age calculations. The $^{207}Pb/^{206}Pb$ ratios were corrected for mass fractionation by a factor of 0.12% per a.m.u., given by repeated analysis of the NBS-982 standard, and analytical uncertainties are given at the 2σ level.

The U–Pb ID-TIMS technique was adapted from Krogh (1973) and Parrish (1987). The zircon crystals were ultrasonically cleaned with methanol and a mixture of diluted HCl + HNO_3. The grains were then dissolved in teflon micro-capsules in two sequential steps, using HF + HNO_3 in the first step, and HCl in the last. In each step, the micro-capsules were put in a Parr-type bomb and heated to 245 °C for 12–14 h in an autoclave. A mixed ^{235}U–^{205}Pb tracer was used for determination of Pb/U isotope ratios and concentrations of Pb and U. Thirteen analyses of the NBS 982 standard yielded the following mean ratios: $^{204}Pb/^{206}Pb = 0.0272162$; $^{207}Pb/^{206}Pb = 0.467013$; $^{208}Pb/^{206}Pb = 0.9998288$. Mass fractionation for Pb was 0.12 and 0.18 a.m.u. for UO_2. Total blanks were <30 pg for Pb and <1 pg for U. Calculations have been made with the PbDat (Ludwig, 1993) and Isoplot (Ludwig, 2001) programs.

Instruments and analytical procedures for zircon U–Pb analyses by LAM-ICP-MS are described in detail in Jackson et al. (2004). Images of the internal structure of polished zircons were obtained using the back-scattered electron/cathodoluminescence (BSE/CL) detector on a Cameca SX50 electron microprobe. Grain mounts containing the samples and standards were then cleaned in 1N HNO_3 prior to analysis to remove surface Pb contamination. Analyses were performed using a New Wave LUV213 laser ablation (LA) sampler that uses a focused laser beam (20–30 μm) to ablate a small amount of a sample, and the ablated material is transported in a He carrier gas to an ICP-MS for isotopic quantification. The ICP-MS used was an Agilent 4500, with detection limits for the elements being typically 10 ppb for a 60-s analysis. Low gas blank ^{208}Pb signals of ca. 30–40 cps were achieved routinely, and

backgrounds were <10 cps for the other elements of interest. Data were acquired on five isotopes as a function of time (ablation depth), and subsequent recognition of isotopic heterogeneity within the ablation volume (e.g., zones of Pb loss or common Pb related to fractures or inclusions, inherited cores, etc.). Each analysis consisted of measurement of instrumental background (i.e., analysis of carrier gas, no ablation) followed by the ablation. Mass discrimination of the mass spectrometer and residual elemental fractionation were corrected by calibration against a standard zircon, GJ-1. Precision is estimated at 1.7–4.1% (2σ), and calculations have been made with the Isoplot program (Ludwig, 2001).

For whole rock Sm–Nd analysis, rock powders were prepared in a ring mill. The powders (∼100mg) were dissolved in a mixture of HF + HNO_3 in teflon bombs at 220 °C for one week. After evaporation, the separation of Sm and Nd was carried out in two steps. Initially, the REE were separated from other elements by cation exchange chromatography, then, Sm and Nd were separated from the REE by anion exchange chromatography. A mixed ^{150}Nd–^{149}Sm spike was used and the Nd data were normalized to a $^{146}Nd/^{144}Nd$ ratio of 0.7219. During the period of analysis, a $^{143}Nd/^{144}Nd$ ratio of 0.511843 ± 12 was obtained for the La Jolla Nd standard. Sm and Nd concentrations for BCR-01 were 6.56 and 28.58 ppm, respectively. Procedural blanks were <110 pg for Sm and <240 pg for Nd. The crustal residence ages were calculated using the values of DePaolo (1988) for the depleted mantle.

4. Single zircon lead evaporation results

4.1. Igarapé Grande Metatonalite

The metatonalite (sample EK32) is a dark gray rock without visible mesoscopic tectonic fabric. Under the microscope, quartz and plagioclase form granoblastic arrays and occur in association with brownish biotite and minor amphibole and K-feldspar. Zircon, apatite, garnet, and opaque minerals are accessory phases, whereas chlorite and white mica are retrometamorphic products. The analyzed zircon crystals are brownish, prismatic, with asymmetric and rounded pyramids. Four crystals yielded spectrometric results in the 1500 °C heating step (Table 2). Three crystals (1, 6, and 11) furnished a mean age of 2594 ± 3 Ma, interpreted as the minimum age of crystallization of the igneous protolith of the metatonalite. The fourth zircon (10) yielded an age of 2662 ± 43 Ma, which is interpreted as inheritance.

4.2. Marajupema Formation

Detrital zircons from a cordierite-bearing feldspathic quartzite (sample EK26) and a quartz–muscovite schist (sample EK33) have been dated. The zircon crystals in these samples show a variety of sizes, morphologies, and degree of roundness. From 31 analyzed crystals of sample EK33, 6 crystals yielded spectrometric results defining at least three age patterns (Table 3). Zircon 2 furnished an Archean age of 2635 ± 47 Ma; zircon 3 yielded a Paleoproterozoic age of 2164 ± 25 Ma; the other four zircons also have Paleoproterozoic ages in the 2016–2084 Ma range. In sample EK26, only 6 out of 58 zircon crystals yielded spectrometric results. These crystals also produced five distinct age patterns, having ages around 1100, 1245, 1690, 1830, and 2140–2160 Ma (Table 3).

5. U–Pb ID-TIMS and LAM-ICPMS results

5.1. Itapeva complex

Sample EK18A (tonalitic gneiss) has previously been dated by the Pb evaporation method (minimum age 2135 ± 4 Ma—Klein and Moura, 2003). Zircons for ID-TIMS U–Pb dating have been separated from the same concentrate used for the Pb evaporation analysis. Five abraded zircon crystals, showing two distinct morphologic patterns, have been analyzed (Fig. 5; Table 4). The

Table 2
Pb evaporation isotope data on zircons from the Igarapé Grande Metatonalite

Zircon	T (°C)	No. of ratios	$^{206}Pb/^{204}Pb$	$^{208}Pb/^{206}Pb$	2σ	$^{207}Pb/^{206}Pb$[a]	2σ	Step age (Ma)	2σ	Mean age (Ma)
EK32—metatonalite										
1	1500	36	5681	0.10792	0.00089	0.17323	0.00045	2589	4	
6	1500	34	>10000	0.14440	0.00058	0.17394	0.00033	2596	3	
11	1500	16	6756	0.14188	0.00058	0.17490	0.00055	2605	5	2594 ± 3[b]
10	1500	6	>10000	0.11417	0.00402	0.18092	0.00467	2662	43	

[a] Corrected according to Stacey and Kramers (1975).
[b] Mean age calculated with crystals 1, 6, and 11.

Table 3
Pb evaporation isotope data on detrital zircons of rocks from the Marajupema Formation

Zircon	T (°C)	No. of ratios	$^{206}Pb/^{204}Pb$	$^{208}Pb/^{206}Pb$[a]	2σ	$^{207}Pb/^{206}Pb$[a]	2σ	Step age (Ma)	2σ
EK33—quartz–muscovite schist									
4	1500	30	>10000	0.05321	0.00079	0.12059	0.00070	1981	8
	1550	8	6060	0.08393	0.00112	0.12839	0.00096	2076	13
5	1500	16	>10000	0.13623	0.00499	0.12048	0.00058	1970	11
	1550	28	>10000	0.12956	0.00501	0.12406	0.00029	2016	4
8	1500	6	>10000	0.04914	0.00071	0.12642	0.00038	2049	5
16	1450	16	3268	0.12974	0.00065	0.12554	0.00049	2037	7
	1500	32	>10000	0.12903	0.00087	0.12854	0.00050	2078	7
	1550	34	>10000	0.13622	0.00037	0.12896	0.00050	2084	7
3	1450	8	>10000	0.11253	0.00329	0.13496	0.00193	2164	25
2	1500	8	>10000	0.14051	0.00127	0.17804	0.00502	2635	47
EK26—quartzite									
1	1500	8	>10000	0.28608	0.00482	0.07256	0.00152	1102	42
10	1500	12	4484	0.09577	0.00109	0.08198	0.00025	1245	6
5	1450	16	3236	0.13904	0.00068	0.11850	0.00047	1830	8
7	1500	8	>10000	0.14566	0.01427	0.10364	0.00218	1691	39
8	1500	12	>10000	0.11249	0.00079	0.13464	0.00084	2159	11
16	1500	16	4425	0.11145	0.00208	0.13317	0.00131	2140	17

[a] Corrected according to Stacey and Kramers (1975).

first group (grains a, b, and i) consists of elongated, prismatic crystals with rounded terminations. Zircons of the second group (grains j and m) are shorter, rather faceted, and rounded. The two groups show also distinct isotopic compositions, with the second group being slightly depleted in U and slightly enriched in Pb compared to the first group (Table 4). In the Concordia diagram (Fig. 5), the three crystals of the first group have isotopic ratios that plot along a straight line. One of the crystals plots on the concordia curve, whereas the two other grains show slight and variable discordance. A regression through these three grains yields a concordia age of 2167.1 ± 2.5 Ma, with MSWD = 0.18 (Fig. 5), which is interpreted as the age of crystallization of the igneous protolith of the gneiss. This result shows that the previous Pb evaporation result was indeed a minimum age. Since the dated gneiss is a rock that experienced a complex evolution (deformation, metamorphism, local migmatization), it is likely that the zircons suffered some Pb loss. We could not relate this Pb loss to a specific event. The isotopic data have been corrected by the Stacey and Kramers (1975) model for the apparent age of 2170 Ma, which was given by the Pb–Pb errochron on the data points (2170 ± 32 Ma, MSWD = 67). In this case, a lower intercept age was not obtained. Changing tentatively the correction of common Pb for the isotopic composition of the concordant zircon, a lower intercept age of 15 Ma is obtained, what would indicate recent Pb loss.

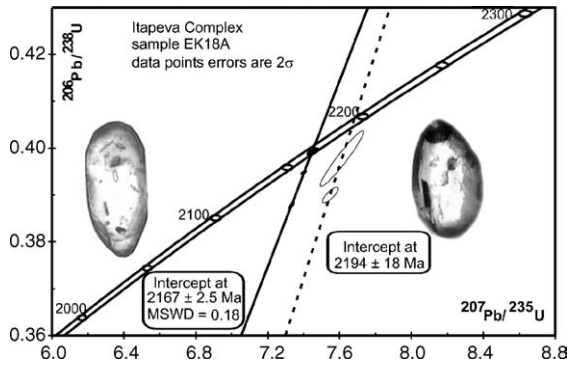

Fig. 5. Concordia plot for zircons of the Itapeva Complex. Image of one zircon of each population is shown for morphologic reference. Data represented by the filled ellipses were used in the age calculation.

The isotopic compositions of the two zircons of the second group do not fit on the above regression line. They plot, with larger errors, in another straight line that intercepts the concordia at 2194 ± 18 Ma (Fig. 5), which is interpreted as inheritance, but they could also reflect two unrelated inherited crystals with distinct ages. We do not have criteria to decide between these two alternatives.

5.2. Maria Suprema Granite

Sample EK25B is a muscovite-bearing granite. The zircon crystals used for ID-TIMS analysis are prismatic

Table 4
Zircon U–Pb isotopes data obtained by ID-TIMS in rocks from the Itapeva Complex and Maria Suprema Granite

Sample/fraction	U (ppm)	Pb (ppm)	Isotope ratios									Apparent ages (Ma)		
			$^{207}Pb/^{204}Pb$	2σ	$^{206}Pb/^{204}Pb$	2σ	$^{206}Pb/^{238}U$[a]	2σ	$^{207}Pb/^{235}U$[a]	2σ	$^{207}Pb/^{206}Pb$[a]	2σ	$^{206}Pb/^{238}U$[a]	$^{207}Pb/^{235}U$[a]	$^{207}Pb/^{206}Pb$[a]
Itapeva Complex															
EK18A															
a	64	38	35.6841	0.427	166.87	0.422	0.399270	0.179	7.45150	0.366	0.13536	0.282	2166	2167	2169
b	78	39	47.5685	0.344	253.59	0.340	0.394789	0.092	7.40126	0.185	0.13597	0.142	2145	2161	2176
i	132	67	51.0571	0.181	276.99	0.167	0.387819	0.159	7.33312	0.193	0.13714	0.103	2113	2153	2191
j	61	43	26.6131	0.312	97.73	0.306	0.397761	1.230	7.61299	1.300	0.13881	0.365	2159	2186	2212
m	56	39	27.0833	0.251	100.16	0.244	0.390002	0.352	7.54851	0.475	0.14038	0.281	2123	2179	2232
Maria Suprema Granite															
EK25A															
358	3104	466	38.5574	0.088	245.977	0.071	0.11998	0.067	1.66885	0.115	0.100879	0.091	730	997	1640
359	1067	233	36.3515	0.107	203.902	0.101	0.16262	0.051	2.50875	0.106	0.111886	0.085	971	1275	1830
386	338	139	68.8457	0.208	434.834	0.186	0.32829	0.221	5.78853	0.257	0.127881	0.127	1830	1945	2069

[a] Corrected according to Stacey and Kramers (1975).

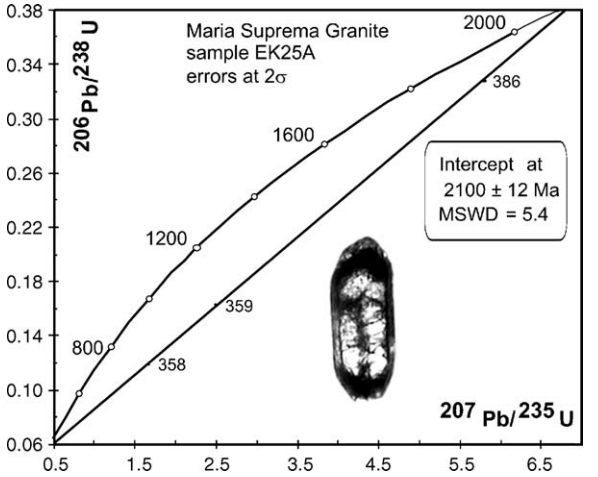

Fig. 6. Concordia plot for zircons of the Maria Suprema Granite. An example of the dated zircons is shown.

with well developed to rather rounded pyramids (Fig. 6), and show a milky aspect produced by metamictization. This alteration made the zircons fragile, and they easily broke during abrasion. To avoid this, it was decided to analyze unabraded crystals. Three crystals (Table 4) produced variably discordant results, as is expected from metamict zircons, since Pb loss might occur as consequence of hydrothermal leaching (Geisler et al., 2001) and/or partial recrystallization (Mezger and Krogstad, 1997). These crystals yielded a discordia line with an upper intercept age of 2100 ± 12 Ma and a lower intercept age of 358 ± 20 Ma (Fig. 6). The upper intercept age is interpreted as the best approximation for the crystallization age of the muscovite-bearing granite, but considering that the zircons are metamictic, this has to be taken as a minimum age. The lower intercept age, despite its imprecision, could be produced by Pb loss due to the imprinting of a Neoproterozoic (500–600 Ma) event (see discussion in Section 8).

5.3. Boca Nova nepheline syenite gneiss

The investigated zircon crystals exhibit, in general, rounded or corroded external forms, suggesting the modification of originally euhedral crystals. Back-scattered electron images (Fig. 7) show that the internal structure of most of the crystals is a mass of irregular bright and dark areas that reflect different concentrations of large heavy ions, especially U and Th. The images also show that the most euhedral crystals retain oscillatory zoning typical of magmatic zircons. Other grains show clear evidence of extensive metamorphic or hydrothermal recrystallization, leaving irregular areas of oscillatory-zoned zircon within a structureless matrix. Most of the zircons

Table 5
Zircon U–Pb (LAM-ICP-MS) data for the Boca Nova Nepheline Syenite Gneiss

Zircon no.	Th (ppm)	U (ppm)	Th/U	Isotope ratios (common Pb corrected)								Apparent ages (Ma)			
				$^{207}Pb/^{206}Pb$	$\pm1\sigma$	$^{207}Pb/^{235}U$	$\pm1\sigma$	$^{206}Pb/^{238}U$	$\pm1\sigma$	$^{208}Pb/^{232}Th$	$\pm1\sigma$	$^{207}Pb/^{206}Pb$	$^{207}Pb/^{235}U$	$^{206}Pb/^{238}U$	$^{208}Pb/^{232}Th$
1	66	2.16	31	0.35891	0.03932	12.247	1.153	0.24748	0.01697	0.03207	0.00047	3745	2624	1425	638
2	866	11.32	77	0.13665	0.00646	3.313	0.148	0.17595	0.00388	0.03711	0.00051	2185	1484	1045	736
4	27	32.42	1	0.06940	0.00227	1.109	0.035	0.11590	0.00172	0.03990	0.00046	911	758	707	791
5R[a]	822	80.62	10	0.06299	0.00123	1.048	0.021	0.12063	0.00157	0.03225	0.00057	708	728	734	642
5C[a]	757	1.73	437	0.06318	0.00085	1.060	0.015	0.12169	0.00144	0.04092	0.00047	714	734	740	811
6	412	118.18	3	0.06217	0.00754	1.018	0.122	0.11876	0.00318	0.03968	0.00044	680	713	723	787
8[a]	512	0.19	2716	0.06306	0.00079	1.071	0.014	0.12321	0.00146	0.03860	0.00045	710	739	749	766
9	417	21.21	20	0.28401	0.06406	6.162	1.295	0.15742	0.01447	0.02749	0.00031	3385	1999	942	548
10	95	0.25	387	0.06687	0.00183	1.069	0.029	0.11601	0.00165	0.03831	0.00046	834	738	708	760
13	96	0.34	281	0.12890	0.02416	2.933	0.533	0.16506	0.00859	0.03270	0.00052	2083	1391	985	650
15	705	0.82	858	0.14124	0.01693	5.611	0.653	0.28820	0.01101	0.03471	0.00044	2242	1918	1633	690
16	264	0.46	575	0.25206	0.01873	6.402	0.429	0.18410	0.00721	0.03275	0.00037	3198	2033	1089	651
17	55	1.29	43	0.10388	0.05205	1.270	0.625	0.08864	0.00893	0.07026	0.00084	1695	833	547	1372
18	2190	104.35	21	0.12633	0.01383	1.737	0.183	0.09967	0.00338	0.02743	0.00040	2048	1022	612	547
19	27	52.21	0.52	0.48374	0.04902	43.927	3.979	0.65922	0.05189	0.07049	0.00096	4192	3864	3264	1377
21[b]	685	1.45	473	0.06116	0.00105	0.904	0.015	0.10720	0.00127	0.03366	0.00058	645	654	656	669
22	935	8.70	107	0.17948	0.01662	3.018	0.257	0.12186	0.00511	0.03652	0.00043	2648	1412	741	725
23A	529	4.62	115	0.08204	0.00317	1.337	0.050	0.11810	0.00198	0.03831	0.00043	1246	862	720	760
23R	24	14.77	1.64	0.09348	0.00470	1.550	0.075	0.12025	0.00242	0.03550	0.00039	1498	950	732	705
24[a]	1547	39.51	39	0.06366	0.00162	1.047	0.027	0.11922	0.00164	0.03700	0.00058	730	727	726	734
26C[a]	192	0.35	542	0.06429	0.00107	1.068	0.018	0.12044	0.00153	0.03967	0.00044	751	738	733	786
26R	10	0.21	50	0.07488	0.03822	1.110	0.563	0.10746	0.00681	0.03415	0.00039	1065	758	658	679
27	2660	25.39	105	0.08452	0.05786	1.322	0.896	0.11347	0.01131	0.03379	0.00081	1305	855	693	672
28	117	0.80	146	0.26427	0.00360	11.610	0.166	0.31872	0.00436	0.01775	0.00020	3272	2573	1783	356
29	1628	1.35	1206	0.08358	0.01364	1.421	0.229	0.12328	0.00387	0.03626	0.00042	1283	898	749	720
30C	20	0.10	198	0.15239	0.01272	3.685	0.287	0.17543	0.00652	0.03825	0.00042	2373	1568	1042	759
30R	599	2.39	250	0.46228	0.07141	18.113	2.384	0.28414	0.02718	0.02928	0.00061	4125	2996	1612	583
31	587	7.41	79	0.31322	0.01267	6.294	0.218	0.14576	0.00397	0.03615	0.00041	3537	2018	877	718

C: core, R: rim.

[a] Concordant spots (used for age calculation = 732 ± 7 Ma; see Fig. 10B).

[b] Concordant zircon (Fig. 10B—see text for explanation).

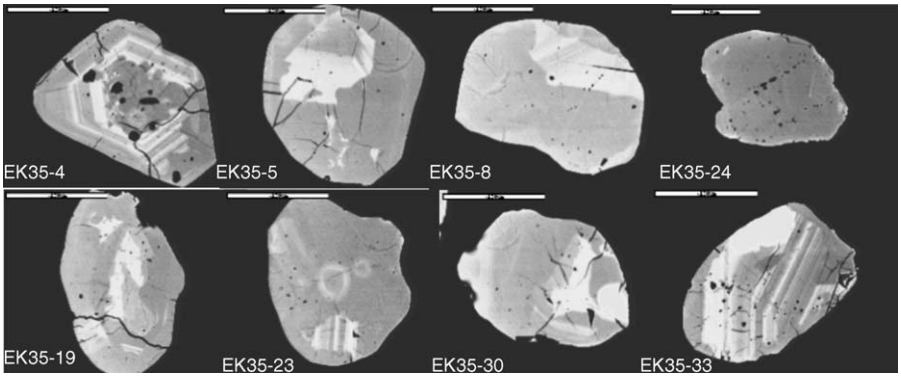

Fig. 7. Back-scattered electron images of zircons of the Boca Nova Nepheline Syenite Gneiss. Crystals in the upper row are concordant. Grains of the lower row are complex, with irregular cores, sometimes showing oscillatory zoning, with structureless overgrowths. Light and dark areas reflect different concentrations of large heavy ions, especially U and Th. Scale bars are 0.1 mm long.

analyzed by LAM-ICP-MS (Table 5) have high Th contents and high Th/U ratio, which is typical of zircons from nepheline syenite (Belousova et al., 2002), whereas other crystals, particularly those showing strong recrystallization, have U contents lower than 1 ppm, which is not characteristic of magmatic rocks, even of nepheline syenite. The concordia diagram (Fig. 8A) shows a cluster of points near concordia with ages between 700 and 750 Ma, and two trends extending toward unrealistically high $^{207}Pb/^{206}Pb$ ages. These trends resemble those produced by common Pb contamination. However, common Pb contamination typically produces $^{208}Pb/^{232}Th$ ages that are $\gg ^{206}Pb/^{238}U$ ages, and most of the $^{208}Pb/^{232}Th$ apparent ages are in the 550–800 Ma range (Table 5). Therefore, the common Pb explanation is improbable. Instead, these trends probable reflect the loss of U, but not Th, from the zircons during the recrystallization. The age of crystallization of the igneous protolith is best constrained by four concordant zircons (Fig. 8B) with an intercept age of 732 ± 7 Ma (5 spots, 95% confidence). This age is very close to the whole rock Rb–Sr isochrone age of 723 ± 30 Ma obtained by Villas (1982). The timing of the recrystallization cannot be well constrained with these data. However, the presence of a single concordant grain at 650 Ma, and the range of $^{208}Pb/^{232}Th$ ages down to 550 Ma, suggest that the hydrothermal recrystallization event occurred within 100–200 Ma of the original igneous crystallization of the protolith, which is all indicated by the K–Ar age in biotite of 580 ± 10 Ma.

6. Sm–Nd isotope results

Sm–Nd isotope compositions have been determined in gneisses of the Itapeva Complex, supracrustal rocks of the Chega Tudo and Marajupema Formations, muscovite–granite of the Maria Suprema unit, and in the Boca Nova nepheline syenite gneiss. The isotopic results

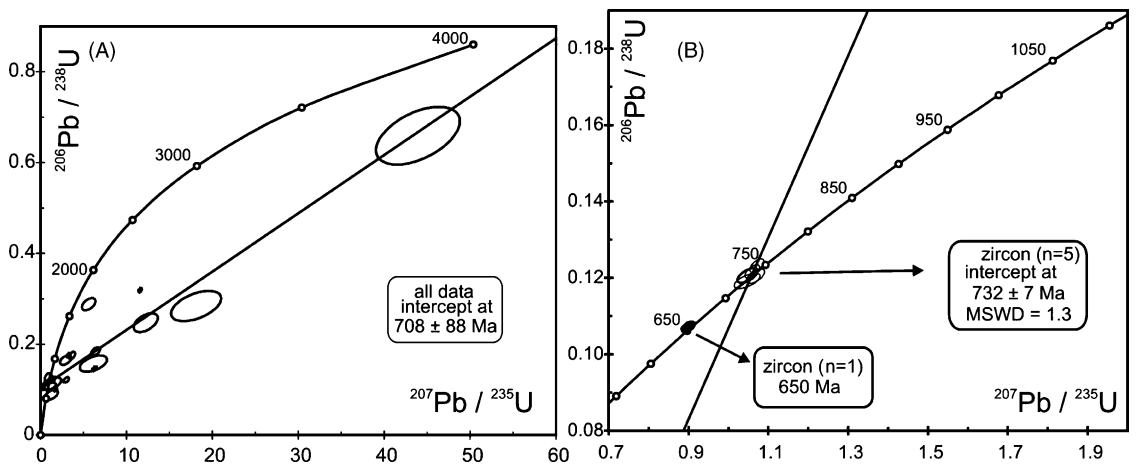

Fig. 8. Concordia plots for zircons of the Boca Nova Nepheline Syenite Gneiss: (A) all data and (B) concordant zircons.

Table 6
Whole rock Sm–Nd isotope results for rocks of the Gurupi Belt

Sample	Rock type	Zircon age (Ma)	Sm (ppm)	Nd (ppm)	f(Sm/Nd)[a]	$^{147}Sm/^{144}Nd$[a] ($\pm1\sigma$)	$^{143}Nd/^{144}Nd$ ($\pm1\sigma$)	ε_{Nd_0}	$\varepsilon_{Nd}(t)$	T_{DM} (Ga)
Itapeva Complex										
EK18A	Tonalite gneiss	2167	2.00	10.88	−0.43	0.11124 ± 13	0.511553 ± 20	−21.2	+2.6	2.22
EK21	Tonalite gneiss	2167	3.08	17.52	−0.46	0.10644 ± 5	0.511423 ± 15	−23.7	+1.4	2.31
Maria Suprema Granite										
EK22	Musc-granite	2100	5.40	45.05	−0.56	0.08592 ± 6	0.511310 ± 5	−25.9	+4.0	2.07
EK25B	Musc-granite	2100	7.15	41.63	−0.47	0.10387 ± 9	0.511390 ± 8	−24.3	+0.7	2.30
Chega Tudo Formation										
MD16	Felsic metav	2160	8.69	40.61	−0.34	0.12942 ± 18	0.511787 ± 5	−16.6	+2.1	2.28
JP49	Felsic metav	2160	9.12	69.01	−0.59	0.07990 ± 18	0.511113 ± 10	−29.7	+2.7	2.20
SD56	C-schist	2160	3.26	16.95	−0.41	0.11607 ± 6	0.511548 ± 10	−21.2	+1.1	2.34
Marajupema Formation										
EK33	Musc-schist	1100[b]	2.66	13.38	−0.39	0.12035 ± 12	0.511572 ± 32	−20.8	−10.1	2.41
EK26	Quartzite	1100[b]	1.01	5.35	−0.42	0.11414 ± 1	0.511726 ± 3	−17.8	−6.2	2.02
EK27	Quartzite	1100[b]	7.31	41.75	−0.46	0.10582 ± 21	0.512047 ± 34	−11.5	+1.3	1.41
Boca Nova Nepheline Syenite Gneiss										
EK35	Neph-syenite	730	1.31	11.49	−0.65	0.06907 ± 5	0.511872 ± 22	−14.9	−2.92	1.24

musc: muscovite, metav: metavolcanic; C: carbon; neph: nepheline.
[a] Normal values for unfractionated felsic rocks (Sato and Siga Jr., 2002): f(Sm–Nd) −0.60 to −0.35; $^{147}Sm/^{144}Nd$ 0.09–0.125.
[b] Modelled for the youngest detrital zircon age.

are reported in Table 6. With one exception (sample EK35), the analyzed samples have $^{147}Sm/^{144}Nd$ ratios and Sm–Nd fractionation factors [f(Sm–Nd)] within, or close to, the accepted range for felsic rocks that have not undergone chemical Sm–Nd fractionation (DePaolo, 1988); the results therefore are suitable for model age determinations.

Two samples of orthogneisses of the Itapeva Complex yielded depleted mantle (T_{DM}) model ages of 2.22 and 2.31 Ga, with ε_{Nd} (t = 2167 Ma) values of +2.6 and +1.4, respectively. The felsic metavolcanic rocks of the Chega Tudo Formation have model ages of 2.20 and 2.28 Ga and ε_{Nd} (t = 2160 Ma) values of +2.7 and +2.1, respectively. These positive ε_{Nd} values and depleted mantle model ages are not significantly older than the crystallization ages of the gneisses and metavolcanic rocks. As such, the rocks of these units are interpreted as being derived from Paleoproterozoic juvenile mantle sources. A graphite-bearing schist of the Chega Tudo Formation provided a slightly older T_{DM} age of 2.34 Ga and an ε_{Nd} value of +1.1. These data also indicate that the detrital sources were predominantly (if not exclusively) of Paleoproterozoic age.

Two samples of muscovite-bearing granite of the Maria Suprema unit show T_{DM} model ages of 2.07 and 2.30 Ga with ε_{Nd} (t = 2100 Ma) values of +4.0 and +0.7, respectively. The peraluminous composition of this granite indicates that it derived from crustal sources or their erosion products, which is reinforced by the model age of sample EK25B (2.30 Ga). This model age probably represents an average of the sources involved. Yet, the positive ε_{Nd} values suggest that Archean sources have not been present, or they have been very subordinate, which is in keeping with the absence of inherited Archean ages in the dated zircons. In this respect, the Maria Suprema Granite differs from the other muscovite-bearing granites (Jonasa, Japiim) in the Gurupi Belt that show strong evidence for the involvement of Archean sources.

Three samples of clastic metasedimentary rocks of the Marajupema Formation gave quite different T_{DM} model ages of 2.41, 2.02, and 1.41 Ga, with ε_{Nd} (t = 1100 Ma) values of −10.1, −6.2, and +1.3, respectively. One of the samples (EK27) shows high Sm and Nd contents, which could reflect the presence of garnet (and possibly other minerals). Since model ages of sedimentary rocks represent an average of the age of the sources of the sediments, these three samples indicate variable detrital sources, having Archean and Paleoproterozoic in addition to Neoproterozoic ages.

The Boca Nova nepheline syenite gives a T_{DM} model age of 1.24 Ga and an ε_{Nd} (t = 730 Ma) value of −2.9. The $^{147}Sm/^{144}Nd$ ratios and Sm–Nd fractionation factor of the nepheline syenite (Table 6) are lower than the normal values accepted for unfractionated rocks. Furthermore, considering the low $^{87}Sr/^{86}Sr$, and the high trace-element (Rb, Sr, Ba, Nb, and Zr) concentrations, mixed mantle-derived and enriched (mantle- or crust-derived) sources have probably been involved in the parental magma of the alkaline rock. Therefore, in this case, depleted mantle or CHUR model ages are meaningless. Moreover, the presence of inherited zircon crystals also indicates that the reworking of older crust played a role in the genesis of the Boca Nova nepheline syenite.

7. Discussion

In the age versus ε_{Nd} diagram (Fig. 9), the compositions of the rocks of the Gurupi Belt form broadly three domains. One Paleoproterozoic domain is composed of calc-alkaline/TTG juvenile rocks formed at 2150–2168 Ma. Another Paleoproterozoic domain is comprised of peraluminous granites formed at 2080–2100 Ma through the reworking of Paleoproterozoic and Archean crustal protoliths. These two domains match those formed by similar and coeval rocks of the São Luís Craton (Fig. 9), and the older one represents the accretion of juvenile crust in the Rhyacian at ca. 2.2 Ga. The third domain indicates the reworking of pre-existing crust during the Neoproterozoic. Part of this is probably the juvenile crust formed in the Rhyacian period (the "São Luís crust", Fig. 9), and part comes from Archean protoliths.

The 12 detrital zircons of the Marajupema Formation that furnished isotopic results (Table 3) yielded 5 distinct groups of ages, broadly around 2.63, 2.16, 2.05–2.08, 1.70, and 1.10–1.20 Ga. The only known source for the Archean zircon is the Igarapé Grande Metatonalite (2.59 and 2.66 Ga). However, other Archean ages have been found in granitic injections (mobilized) in the Itapeva Complex (2.58 and 2.61 Ga—Klein and Moura, 2003). The two older groups of Paleoproterozoic zircons correspond to well defined sources in the region, which are the calc-alkaline granitoids (Tromaí Suite, Itapeva Complex, Cantão and Areal granites) and volcanic rocks (Chega Tudo Formation) of 2150–2168 Ma, and the peraluminous granites (Maria Suprema, Japiim, Tracuateua, Jonasa) of 2070–2100 Ma. The two latter groups come from sources not yet detected in the study area. Since we do not have means to evaluate the degree of discordance of these zircons, we do not know whether these ages are significant or whether the zircons suffered some lead loss after their formation. However, it is worth noting that the sample that contains the younger zircon (ca. 1100 Ma) has also a positive ε_{Nd} value, indicating that a substantial

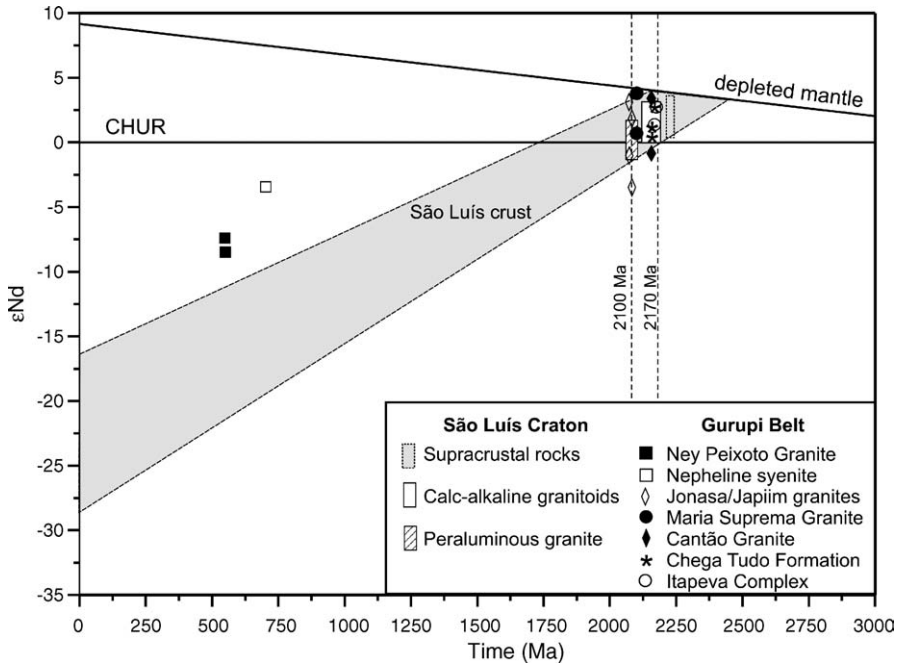

Fig. 9. Time vs. ε_{Nd} diagram for the rocks of the Gurupi Belt (data from this study and from Palheta, 2001; see text and tables). The fields occupied by the rocks of the São Luís Craton are shown for comparison (data from Palheta, 2001; Klein et al., 2005). Note that most of the Paleoproterozoic rocks of the Gurupi Belt and São Luís Craton are enveloped by the shaded area labeled "São Luís crust".

amount of the detritus came from source rocks probably younger than 1100 Ma. Therefore, despite the small number of analyses, it is clear that these rocks represent a sedimentary basin with a maximum depositional age around 1100 Ma.

8. Geodynamic evolution and concluding remarks

Information on field relationships (scarce), rock association and geochemistry, and geochronological (zircon, Rb–Sr, and K–Ar) and Nd isotope data provide some insights into the tectonic settings and geodynamic evolution of the Gurupi Belt. It has become clear that this belt is the result of a poly-phase evolution with magmatic activity taking place in at least five events: ~2600 Ma (Neoarchean), 2167–2148 Ma (early Rhyacian), 2100–2080 Ma (late Rhyacian), 730 Ma (Cryogenian), and 550 Ma (Neoproterozoic III). Among these, the Neoarchean event is not yet characterized; the early Rhyacian rocks are clearly related to an episode of crustal growth that is well defined in the São Luís Craton; the late Rhyacian rocks are related to a collision event; the Cryogenian rock is related to a rift event; the Neoproterozoic III rock is a peraluminous, probably post-tectonic granite. In addition, other ages or age intervals that have not yet been recognized as events have been detected in detrital and inherited zircons.

8.1. The Archean and Paleoproterozoic scenarios

The Archean in the region is represented only by the Igarapé Grande Metatonalite and is also recorded in detrital zircons, and in inherited zircons and model ages of Paleoproterozoic and Neoproterozoic units. Therefore, the Archean rocks were present mostly as vestiges of an older continent that participated in the Proterozoic evolution of the Gurupi Belt.

A considerable part of the lithologic framework of the belt formed between 2168 and 2080 Ma, and parts of these Paleoproterozoic terranes are continuous with the Paleoproterozoic units of the present-day São Luís Craton. Klein et al. (2005) interpreted the cratonic units, mostly formed at 2168–2150 Ma, as representing accretionary (juvenile) assemblages developed in intra-oceanic island arcs (Fig. 10A). The reworking (erosion and partial melting) of the island arcs produced volcano–sedimentary and sedimentary sequences deposited in the margins or depressions of the arcs, along with more evolved granites (Fig. 10A). The metavolcano–sedimentary Chega Tudo Formation, and the sedimentary Gurupi Group, may represent

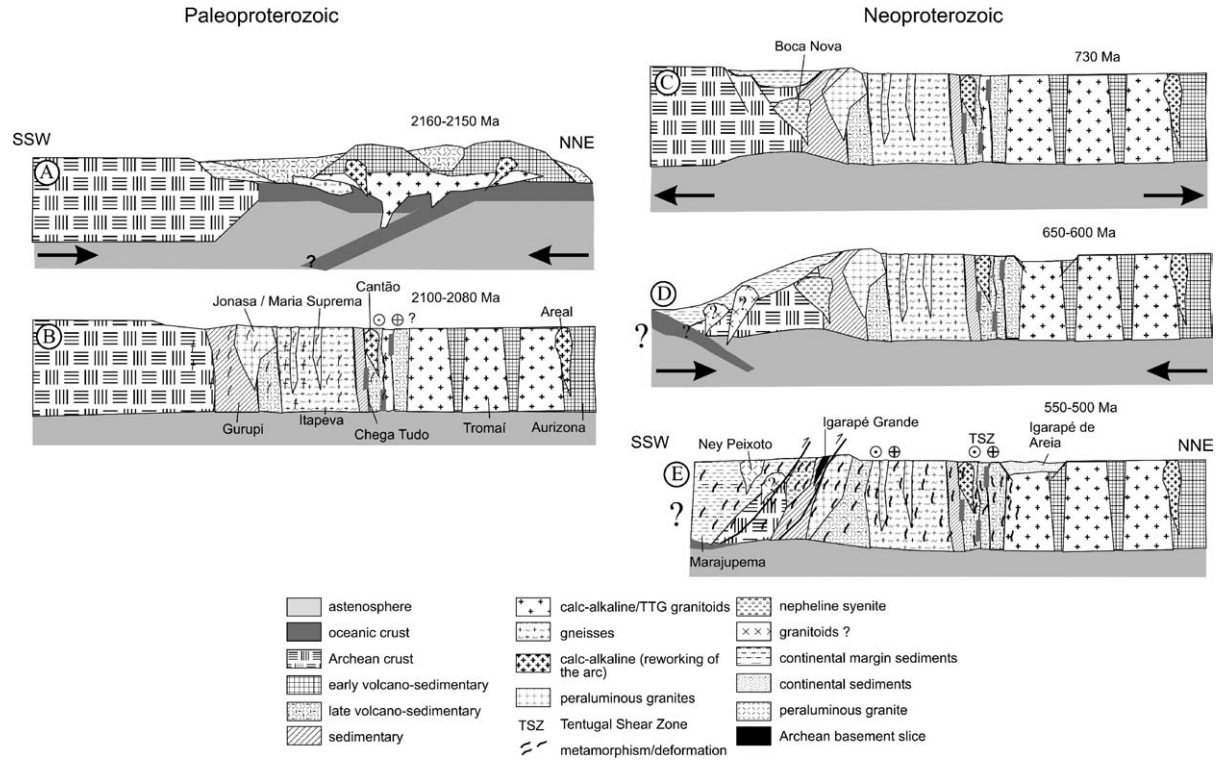

Fig. 10. Schematic (not to scale) cross-sections illustrating the proposed geodynamic evolution of the Gurupi Belt and the nearby São Luís Craton (see text for detailed discussion). (A) Paleoproterozoic accretionary phase. Opening of an oceanic basin, formation of intra-oceanic island arcs, onset of subduction producing calc-alkaline magmatism, and concomitant reworking (erosion and partial melting) of the island arc. (B) Paleoproterozoic collision of the intra-oceanic island arc with an Archean continent, producing deformation, crustal thickening, amphibolite facies metamorphism, and peraluminous granites. (C) Rifting of the crust amalgamated in the Paleoproterozoic, deposition of continental immature sediments, and intrusion of the nepheline syenite. (D) Evolution of the continental rift probably to a continental margin, sedimentation, subduction (?), and production of felsic magmatism. (E) Closure of the orogenic basin and collision, with thickened crust producing metamorphism, deformation, and partial melting.

these types of successions (back-arc, fore-arc basins?), whereas the ultramafic lenses intercalated within the Chega Tudo Formation may represent fragments of the subducted oceanic plate or of the rocks that floored the marginal basins. In addition, the tonalitic gneisses of the Itapeva Complex (2167 Ma) are likely part of the major arc-related calc-alkaline magmatism that formed the roots of the arcs, and the Cantão Granite (2159 Ma) is one of the evolved granites (Fig. 10B).

In the Gurupi Belt, the presence of several bodies of Paleoproterozoic muscovite-bearing granites brings also insights into the tectonic setting. These granites are considered to be produced in a collisional setting, and their emplacement is interpreted as resulting from crustal thickening by frontal and/or oblique collision (e.g., Brown, 1994; Barbarin, 1996; Solar et al., 1998), as a consequence of the thermal relaxation and/or exhumation of the orogen, after the metamorphic peak (England and Thompson, 1984). Among these peraluminous granites, the Maria Suprema Granite (2100 ± 12 Ma) is clearly syntectonic, whereas the Jonasa, Ourém, and Japiim plutons probably are late- to post-tectonic (Fig. 3). The gneissic fabric and some folding that accompanied the amphibolite-facies metamorphism of the Itapeva Complex developed to accommodate shortening due to crustal thickening during continental collision. This was probably followed by transcurrent tectonics. Alternatively, models that invoke a strike–slip regime are also employed to explain the generation and emplacement of peraluminous granitoids (e.g., Delor et al., 2003; Naba et al., 2004). In both cases, they broadly mark the suture zone and constrain the approximate age of the regional metamorphism and the collisional episode.

The peraluminous granites, the moderate migmatization, the inherited Archean zircons and Archean model ages, and some negative ε_{Nd} values in several Paleoproterozoic units of the Gurupi Belt, are all evidence of variable degrees of reworking of pre-existing crust, in contrast to the juvenile character encountered in the São

Luís Craton. These lines of evidence strongly indicate that an Archean continent existed to the south–southwest (Fig. 10A), and that the Paleoproterozoic calc-alkaline and supracrustal rocks have been amalgamated to the margin of this Archean block, with convergence occurring from north–northwest to south–southwest (Fig. 10A and B). This pre-existing continent is still of unknown derivation and might be represented by Archean portions of the Amazonian Craton or by the concealed Parnaíba Block (Fig. 2), or by an unknown crustal block. Considering the good correlation of the Paleoproterozoic sequences with the rocks of the West African Craton that have been affected by the Eburnean orogeny, another possibility would be the collision against an Archean portion of the West African Craton. In this case, however, this could imply significant rotation of the present-day position of the São Luís Craton and Gurupi Belt, and we do not have means to discuss this.

The Paleoproterozoic orogenic events that are recorded in the Gurupi Belt and in the adjacent São Luís Craton appear to represent the two end members of orogenesis (accretionary and collisional) that operated in the Paleoproterozoic (e.g., Windley, 1992; Condie, 1997; Kröner and Cordani, 2003). Accordingly, the evolution of the São Luís Craton (and part of the Gurupi Belt) resembles the accretionary orogenies that are characterized by the agglutination of juvenile oceanic terranes (island arcs, for instance), without significant crustal thickening, leading to low-grade metamorphism. The climax of this event is represented by the large-scale calc-alkaline magmatism that occurred especially at 2170–2150 Ma. On the other hand, in the Paleoproterozoic portion of the Gurupi Belt, the reworking of pre-existing crust has been documented, and crustal thickening is strongly suggested by partial melting, localized migmatization and amphibolite-facies metamorphism, implying a collisional event at 2100–2080 Ma. These two peaks of activity are widespread in the South American continent and are treated as different orogenies of the same cycle (Hartmann, 2002; Santos et al., 2003) or as a single and continuous orogenic event, involving continental break-up, opening of an oceanic basin, built-up of arc systems, and collision of the arcs against a continental margin (Delor et al., 2003), i.e., a soft collision followed by a hard collision.

8.2. The Neoproterozoic scenario

The geodynamic evolution of the Gurupi Belt in the Neoproterozoic must take into account, in addition to the petrologic and structural evidence, the following geochronological information: (1) the crystallization ages of the Boca Nova nepheline syenite and the Ney Peixoto granite; (2) the age of the detrital zircons found in the Marajupema and Igarapé de Areia formations; (3) the occurrence of Neoproterozoic (ca. 800–550 Ma) Rb–Sr and K–Ar mineral ages in several Paleoproterozoic units.

After the Paleoproterozoic collage, the next event that is clearly identified in the region was the intrusion of the Boca Nova nepheline syenite 732 Ma ago, recording the rifting of a pre-existing crust (Fig. 10C). This anorogenic intrusion has subsequently been deformed and metamorphosed under amphibolite-facies conditions, indicating that the rift that also received the sediments of the Marajupema Formation has eventually been closed. Two possibilities (not unique) are envisaged for the evolution of this rift: (1) it evolved as an aborted continental rift, characterizing an intracontinental orogen; (2) a continental margin/oceanic basin formed as spreading followed after rifting, with subsequent development of subduction (arcs?) and collision (Fig. 10C). It is noteworthy that the Igarapé de Areia Formation (the sedimentary basin deposited over rocks of the São Luís Craton close to its limit with the Gurupi Belt) is composed of immature (arkosic) sediments, indicating the proximity of the source areas, and that more than 80% of the analyzed detrital zircons of this formation have ages in the 600–650 Ma range (Pinheiro et al., 2003). Considering that felsic to intermediate rocks are the main sources of detrital feldspars and zircons to sediments, it is possible to infer that felsic–intermediate (orogenic/anorogenic?) magmatism has to some extent occurred in the region around 600–650 Ma, even though it has not yet been recognized. This magmatism might be concealed beneath the Phanerozoic cover or it has already been eroded away. It must be emphasized that two of the three occurrences of Neoproterozoic rocks (Boca Nova Nepheline Syenite Gneiss and Marajupema Formation) were metamorphosed in the amphibolite facies and that a considerable part of the overlying crust has already been removed from the geological record. Recent studies, based on geological, geochronological, and paleomagnetic evidence (Pimentel et al., 1999; Caby, 2003; Cordani et al., 2003; Fetter et al., 2003; Kröner and Cordani, 2003), strongly suggest that a large Neoproterozoic (Brasiliano/Pan-African) ocean existed between central South America and the eastern margin of the West African Craton. This hints the hypothesis that the continental rift in the Gurupi region evolved to an oceanic basin (Fig. 10D) that could be a branch of the large Brasiliano/Pan-African ocean. As an alternative explanation, both zircons and other detritus could have originated from anorogenic (pre-orogenic) magmatism, and thus an intracontinental orogeny could be invoked.

Despite the fact that the closure of an orogenic basin in the Neoproterozoic, as part of the Brasiliano/Pan-African cycle of orogenies, is strongly supported by our data, the precise age of this closure and of the accompanying metamorphism and deformation is, however, unconstrained. Available Rb–Sr and K–Ar whole rock and mineral ages of several Paleoproterozoic units span from 1000 to 520 Ma, mostly from 580 to 520 Ma (see Table 1), and the U–Pb system in zircon of the Paleoproterozoic Maria Suprema Granite appears to reflect Pb loss, indicating that these units have been reworked in the Neoproterozoic becoming the basement units in the external portion of the Brasiliano belt. We do not know if all these ages represent metamorphic or cooling ages, or if they partially reflect late strike–slip movements. Field evidence suggests that the peraluminous Ney Peixoto Granite (crystallization age of 549 Ma) is post-tectonic. As such, one can envisage the metamorphism and deformation as being older than this granite, occurring more probably between 580 and 550 Ma. A feature that is clearly related to this tectonic event is the development of moderate- to low-angle structures indicating a tectonic polarity toward the São Luís Craton. These structures affect, among other units, the Marajupema Formation and the Boca Nova nepheline syenite, which are Neoproterozoic units. Dating, in a future work, of suitable minerals associated with these structures can resolve this issue. The Piriá and Igarapé de Areia sedimentary basins probably formed during the exhumation of the orogen, since their rocks still record some deformation and anchimetamorphism, representing the post-orogenic (molassic type?) sequences.

8.3. The Tentugal shear zone and the Neoproterozoic suture

The interpretation of the Tentugal shear zone as a suture between the São Luís Craton and the Gurupi Belt (e.g., Hasui et al., 1984; Abreu and Lesquer, 1985) is not straightforward. This interpretation has relied on limited structural and geophysical data, but our review and new data can contribute to this discussion. The gravity contrasts across the structure are not large (mean Bouguer values of +30 and +10 mGal; Lesquer et al., 1984), if compared to typical suture zones (e.g., Scarrow et al., 2002; Bierlein and Betts, 2004), and typical ophiolites and high-pressure assemblages have not been described in the region. This gravity contrast could be explained by density contrasts produced by the presence of mafic and ultramafic bodies intercalated within the metavolcano–sedimentary rocks of the Chega Tudo Formation, or by the juxtaposed amphibolite-facies gneisses (Itapeva Complex) and greenschist-facies metavolcano–sedimentary rocks (Chega Tudo Formation). However, it is possible that granulite facies rocks underlie the gneisses. Furthermore, rocks of the same age and Sm–Nd signature crop out on both sides of the shear zone, but they have distinctive Rb–Sr and

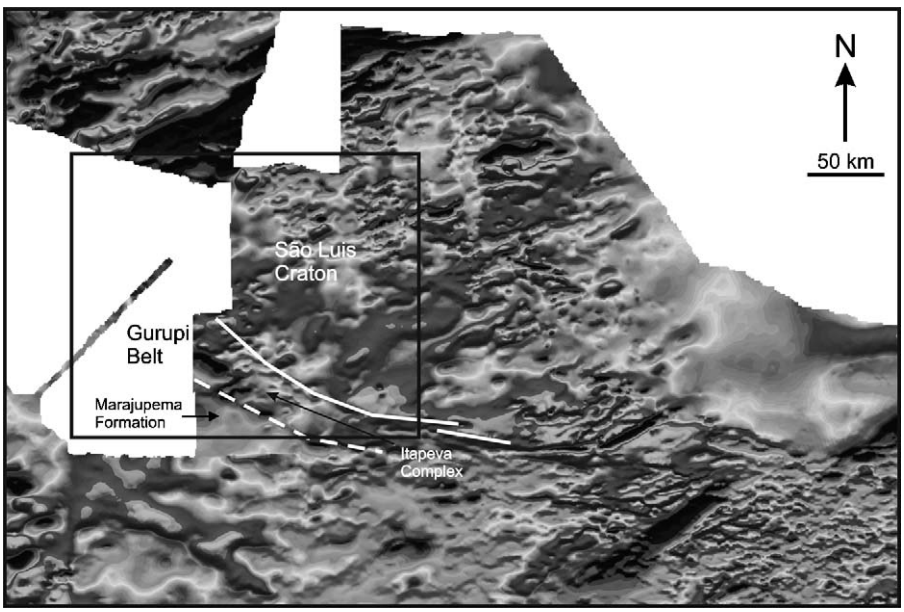

Fig. 11. Magnetic map (total field) of the Gurupi region. Observe the contrasting patterns in the contact zone (dashed line) between the Mesoproterozoic/Neoproterozoic Marajupema Formation (metasedimentary) and the Paleoproterozoic Itapeva Complex (gneisses). The solid lines mark the position of the Tentugal shear zone, and the rectangle corresponds to that of Fig. 3.

K–Ar patterns. Moreover, magnetic contrasts are sharper to the south, in the contact zone between the gneissic massif of the Paleoproterozoic Itapeva Complex and the Neoproterozoic–Mesoproterozoic metasedimentary rocks of the Marajupema Formation (Fig. 11). Therefore, we interpret the Tentugal shear zone as the geochronological boundary between the São Luís Craton and the Gurupi Belt, but not as a suture. The Neoproterozoic suture is more probably located to the south, being approximately marked by the Boca Nova Nepheline Syenite Gneiss, and by the magnetic contrast. It is known (Burke et al., 2003) that if alkaline rocks are involved in an orogenic episode, they undergo metamorphism and deformation and will indicate the proximity of suture zones. The overall evolution of the Tentugal shear zone is also unconstrained, especially if it has been active in the Paleoproterozoic. It should be emphasized that a better understanding of the evolution of the Tentugal shear zone is highly desirable, because of the metallogenic importance of this zone, given its spatial association with most (perhaps all) known gold deposits of the Gurupi Belt. This knowledge is critical for the development of genetic models.

Acknowledgements

Thomas Scheller, Valter Gama Avelar, Marco Antonio Galarza, Rosemary Brabo Monteiro, Elma Oliveira, and Roberta Florencio are greatly acknowledged for technical support during the analytical work at UFPA. Suzy Elhlou and Norman Pearson provided much help during the U–Pb analyses at Macquarie University. Comments by J.M. Lafon, B.B. Brito Neves, R.N.N. Villas, and A. Giret on an early version of the manuscript are much appreciated. We are grateful to Dr. U.G. Cordani and an anonymous reviewer for their comments and suggestions. Contribution to the project 66.2103/1998 PRONEX/CNPq/UFPA (www.ufpa.br/cg/pronex/pronex) and contribution no. 416 from the ARC National Key Centre for Geochemical Evolution and Metallogeny of Continents (www.els.mq.edu.au/GEMOC) are greatly acknowledged.

References

Abreu, F.A.M., Villas, R.N.N., Hasui, Y., 1980. Esboço estratigráfico do Precambriano da região do Gurupi, Estados do Pará e Maranhão. In: 31st Congresso Brasileiro de Geologia, Anals, vol. 2, pp. 647–658.

Abreu, F.A.M., Lesquer, A., 1985. Considerações sobre o Pré-Cambriano da região sul-sudoeste do Cráton São Luís. In: 2nd Simpósio de Geologia da Amazônia, Anals, vol. 1, pp. 7–21.

Almaraz, J.S.U., Cordani, U.G., 1969. Delimitação entre as Províncias Geocronológicas Pré-Cambrianas ao longo do Rio Gurupi. In: 23 Congresso Brasileiro de Geologia, Resumo das Conferências e Comunicações, Boletim Especial, vol. 1.

Almeida, F.F.M., Melcher, G.C., Cordani, U.G., Kawashita, K., Vandoros, P., 1968. Radiometric age determinations from northern Brazil. Boletim da Sociedade Brasileira de Geologia 17, 3–14.

Almeida, F.F.M., Hasui, Y., Brito neves, B.B., 1976. The Upper Precambrian of South America, vol. 7. Boletim Instituto de Geociências USP, pp. 45–80.

Almeida, H.G.G., 2000. Programa Levantamentos Geológicos Básicos do Brasil. Programa Grande Carajás. São Luís, folha SA.23, escala 1:1.000.000. Estados do Pará e Maranhão, Brasília, CPRM (CD-ROM).

Barbarin, B., 1996. Genesis of the two main types of peraluminous granitoids. Geology 24, 295–298.

Bartlett, J.M., Dougherty-Page, J.S., Harris, N.B.W., Hawkesworth, C.J., Santosh, M., 1998. The application of single zircon evaporation and model Nd ages to the interpretation of polymetamorphyc terrains: an example from the Proterozoic mobile belt of south India. Contrib. Mineral. Petrol. 131, 181–195.

Belousova, E., Griffin, W., O'Reilly, S., Fisher, N., 2002. Igneous zircons: trace element composition as an indicator of source rock type. Contrib. Mineral. Petrol. 143, 602–622.

Bierlein, F.P., Betts, P.G., 2004. The Proterozoic Mount Isa Fault Zone, northeastern Australia: is it really a ca. 1.9 Ga terrane-bounding suture? Earth Planet. Sci. Lett. 225, 279–294.

Brito Neves, B.B., Fuck, R.A., Cordani, U.G., Thomaz Filho, A., 1984. Influence of basement structures on the evolution of the major sedimentary basins of Brazil: a case of tectonic heritage. J. Geodyn. 1, 495–510.

Brito Neves, B.B., Santos, E.J., Van Schmus, W.R., 2000. Tectonic history of the Borborema Province. In: Cordani, U.G., Milani, E.J., Thomaz Filho, A., Campos, D.A. (Eds.), Tectonic Evolution of South America, pp. 151–182.

Brown, M., 1994. The generation, segregation, ascent and emplacement of granite magma: the migmatite-to-crustally-derived granite connection in thickened orogens. Earth Sci. Rev. 36, 83–130.

Burke, K., Ashwal, L.D., Webb, S.J., 2003. New way to map old sutures using deformed alkaline rocks and carbonatites. Geology 31, 391–394.

Caby, R., 2003. Terrane assembly and geodynamic evolution of central–western Hoggar: a synthesis. J. Afr. Earth Sci. 37, 133–159.

Condie, K.C., 1997. Plate Tectonics and Crustal Evolution. Heinemann, Oxford, Butterworth, 282 pp.

Cordani, U.G., Melcher, G.C., Almeida, F.F.M., 1968. Outline of the Precambrian geochronology of South America. Can. J. Earth Sci. 5, 629–632.

Cordani, U.G., Sadowski, G.R., Almaraz, J.S., 1974. Estudo geocronológico do Cráton de São Luís. Anais da Academia Brasileira de Ciências 46, 702.

Cordani, U.G., Brito Neves, B.B., Fuck, R.A., Porto, R., Thomaz Filho, A., Cunha, F.M.B., 1984. Estudo preliminar de integração do Pré-Cambriano com os eventos tectônicos das bacias sedimentares brasileiras Explor. Petrobras 15, 70 pp.

Cordani, U.G., D'Agrella Filho, M.S., Brito Neves, B.B., Trindade, R.I.F., 2003. Tearing up Rodinia: the Neoproterozoic palaeogeography of South American cratonic fragments. Terra Nova 15, 350–359.

Costa, J.B.S., Pastana, J.M.N., Costa, E.J.S., Jorge-João, X.S., 1988. A faixa de cisalhamento Tentugal na Folha SA.23-Y-B. In: 35 Congresso Brasileiro de Geologia, Anals, vol. 5, pp. 2257–2266.

Costa, J.L., 2000. Programa Levantamentos Geológicos Básicos do Brasil. Programa Grande Carajás. Castanhal, Folha SA. 23-V-C. Estado do Pará, Belém, CPRM (CD-ROM).

Costa, J.L., Araujo, A.A.F., Villas Boas, J.M., Faria, C.A.S., Silva Neto, C.S., Wanderley, V.J.R., 1977. Projeto Gurupi, DNPM/CPRM, 258 pp.

Cunha, F.M.B., 1986. Evolução paleozóica da Bacia do Parnaíba e seu arcabouço tectônico. M.Sc. Thesis. Universidade Federal do Rio de Janeiro, Instituto de Geociências, 107 pp.

Delor, C., Egal, E., Lafon, J.M., Cocherie, A., Guerrot, C., Rossi, P., Truffert, C., Théveniaut, H., Phillips, D., Avelar, V.G., 2003. Transamazonian Crustal Growth and Reworking as Revealed by the 1:500,000-Scale Geological Map of French Guiana, second ed. Géologie de la France 2-3-4, pp. 5–57.

DePaolo, D.J., 1988. Neodymium Isotope Geochemistry. An Introduction. Springer-Verlag, Berlin.

Dias, G.S., 1983. Estudo petrológico da seqüência vulcanossedimentar de Chega Tudo, região do Gurupi, Estado do Maranhão. B.Sc. Monograph. Universidade Federal do Pará, Departamento de Geologia, Belém, 42 pp.

England, P.C., Thompson, A.B., 1984. Pressure–temperature–time paths of regional metamorphism I. Heat transfer during the evolution of regions of thickened continental crust. J. Petrol. 25, 894–928.

Fetter, A.H., Santos, T.J.S., Van Schmus, W.R., Hackspacher, P.C., Brito Neves, B.B., Arthaud, M.H., Nogueira Neto, J.A., Wernick, E., 2003. Evidence for Neoproterozoic continental arc magmatism in the Santa Quitéria Batholith of Ceará State, NW Borborema Province, NE Brazil: implications for the assembly of West Gondwana. Gondwana Res. 6, 265–273.

Geisler, T., Ulonska, M., Schleicher, H., Pidgeon, R.T., van Bronswijk, W., 2001. Leaching and differential recrystallization of metamict zircon under experimental hydrothermal conditions. Contrib. Mineral. Petrol. 141, 53–65.

Gorayeb, P.S.S., Gaudette, H.E., Moura, C.A.V., Abreu, F.A.M., 1999. Geologia e geocronologia da Suíte Rosário, nordeste do Brasil, e sua contextualização geotectônica. Revista Brasileira de Geociências 29, 571–578.

Hartmann, L.A., 2002. The Mesoproterozoic supercontinent Atlantica in the Brazilian Shield—review of geological and U–Pb zircon and Sm–Nd isotopic evidence. Gondwana Res. 5, 157–163.

Hasui, Y., Abreu, F.A.M., Villas, R.N.N., 1984. Província Parnaíba. In: O Pré-Cambriano no Brasil. Edgard Blücher, São Paulo, pp. 36–45.

Hurley, P.M., Almeida, F.F.M., Melcher, G.C., Cordani, U.G., Rand, J.R., Kawashita, K., Vandoros, P., Pinson, W.H., Fairbairn, H.W., 1967. Test of continental drift by comparison of radiometric ages. Science 157, 495–500.

Hurley, P.M., Melcher, G.C., Pinson, W.H., Fairbairn, H.W., 1968. Some orogenic episodes in South America by K–Ar and whole-rock Rb–Sr dating. Can. J Earth Sci. 5, 633–638.

Jackson, S.E., Pearson, N.J., Griffin, W.L., Belousova, E.A., 2004. The application of laser ablation-inductively coupled plasma-mass spectrometry to in situ U–Pb zircon geochronology. Chem. Geol. 211, 47–69.

Jorge-João, X.S., 1980. O Litchfieldito Boca Nova no nordeste do Estado do Pará: aspectos petroquímicos e implicação econômica. Internal Report. CPRM, Belém.

Klein, E.L., 2004. Evolução crustal pré-cambriana e aspectos da metalogênese do ouro do Cráton São Luís e do Cinturão Gurupi, NE-Pará/NW-Maranhão, Brasil. Unpublished D.Sc. Thesis. Centro de Geociências, Universidade Federal do Pará, 303 pp.

Klein, E.L., Moura, C.A.V., 2001. Age constraints on granitoids and metavolcanic rocks of the São Luís Craton and Gurupi Belt, northern Brazil: implications for lithostratigraphy and geological evolution. Int. Geol. Rev. 43, 237–253.

Klein, E.L., Moura, C.A.V., 2003. Síntese geológica e geocronológica do Cráton São Luís e do Cinturão Gurupi na região do Rio Gurupi (NE-Pará/NW-Maranhão). Geol. USP 3, 97–112.

Klein, E.L., Moura, C.A.V., Pinheiro, B.L.S., 2005. Paleoproterozoic crustal evolution of the São Luís Craton, Brazil: evidence from zircon geochronology and Sm–Nd isotopes. Gondwana Res. 8, 177–186.

Kober, B., 1986. Whole-grain evaporation for $^{207}Pb/^{206}Pb$-age-investigations on single zircons using a double-filament source. Contrib. Mineral. Petrol. 93, 482–490.

Kober, B., 1987. Single grain evaporation combined with Pb + emitter bedding for $^{207}Pb/^{206}Pb$ investigations using thermal ion mass spectrometry, and implications for zirconology. Contrib. Mineral. Petrol. 96, 63–71.

Krogh, T.E., 1973. A low contamination method for hydrothermal decomposition of zircons and extraction of U and Pb for isotopic age determinations. Geochim. Cosmochim. Acta 37, 485–494.

Kröner, A., Jaeckel, P., Williams, I.S., 1994. Pb-loss patterns in zircons from a high-grade metamorphic terrain as revealed by different dating methods: U–Pb and Pb–Pb ages for igneous and metamorphic zircons from northern Sri Lanka. Precambrian Res. 66, 151–181.

Kröner, A., Cordani, U.G., 2003. African, southern India and South American cratons were not part of the Rodinia supercontinent: evidence from field relationships and geochronology. Tectonophysics 375, 325–352.

Lesquer, A., Beltrão, J.F., Abreu, F.A.M., 1984. Proterozoic links between northeastern Brazil and West Africa: a plate tectonic model based on gravity data. Tectonophysics 110, 9–26.

Lowell, G.R., Villas, R.N.N., 1983. Petrology of nepheline syenite gneiss from Amazonian Brazil. Geol. J. 18, 53–75.

Ludwig, K.R., 1993. PBDAT. A Computer Program for Processing Pb–U–Th Isotope Data. Version 1.24. USGS Open File Report 88-542, 34 pp.

Ludwig, K.R., 2001. User's Manual for Isoplot/Ex Version 2.49. A Geochronological Toolkit for Microsoft Excel. Berkeley Geochronology Center, Berkeley, CA, USA, 59 pp. (Special Publication, 1a).

Mezger, K., Krogstad, E.J., 1997. Interpretation of discordant U–Pb zircon ages: an evaluation. J. Metam. Geol. 15, 127–140.

Möller, A., O'Brien, P.J., Kennedy, A., Kröner, A., 2003. The use and abuse of Th–U ratios in the interpretation of zircon. Geophys. Res. Abstr. 5, 12113.

Naba, S., Lompo, M., Debat, P., Bouchez, J.L., Béziat, D., 2004. Structure and emplacement model for late-orogenic Paleoproterozoic granitoids: the Tenkodogo–Yamba elongate pluton (Eastern Burkina Faso). J. Afr. Earth Sci. 38, 41–57.

Nunes, K.C., 1993. Interpretação integrada da Bacia do Parnaíba com ênfase nos dados aeromagnéticos. In: 2nd Congresso Internacional da Sociedade Brasileira de Geofísica, Resumos Expandidos, vol. 1, pp. 152–157.

Palheta, E.S.M., 2001. Evolução geológica da região nordeste do Estado do Pará com base em estudos estruturais e isotópicos de granitóides. M.Sc. Thesis. Centro de Geociências, Universidade Federal do Pará, 143 pp.

Parrish, R.R., 1987. An improved micro-capsule for zircon dissolution in U–Pb geochronology. Chem. Geol. 66, 99–102.

Pastana, J.M.N., 1995. Programa Levantamentos Geológicos Básicos do Brasil. Programa Grande Carajás. Turiaçu/Pinheiro, folhas SA.23-V-D/SA.23-Y-B. Estados do Pará e Maranhão, Brasília, 205pp., CPRM.

Pimentel, M.M., Fuck, R.A., Botelho, N.F., 1999. Granites and the geodynamic history of the Neoproterozoic Brasilia belt, central Brazil: a review. Lithos 46, 463–483.

Pinheiro, B.L.S., Moura, C.A.V., Klein, E.L., 2003. Estudo de proveniência em arenitos das formações Igarapé de Areia e Viseu, nordeste do Pará, com base em datação de monocristais de zircão por evaporação de chumbo. In: 8th Simpósio de Geologia da Amazônia, Resumos Expandidos (CD-ROM).

Ribeiro, J.W.A., 2002. O arcabouço estrutural da região de Chega Tudo e Cedral, NW do Maranhão, com base em sensores geofisicos. M.Sc. Thesis. Universidade Federal do Pará, Belém, Brazil, 155 pp.

Sadowski, G.R., 2000. The São Luís Craton and the Gurupi Fold Belt. In: Cordani, U.G., Milani, E.J., Thomaz Filho, A., Campos, D.A. (Eds.), Tectonic Evolution of South America, pp. 97–99.

Santos, J.O.S., Hartmann, L.A., Bossi, J., Campal, N., Schipilov, A., Piñeyro, D., McNaughton, N.J., 2003. Duration of the Trans-Amazonian cycle and its correlation within South-America based on U–Pb SHRIMP geochronology of the La Plata Craton, Uruguay. Int. Geol. Rev. 45, 27–48.

Sato, K. 1998. Evolução crustal da Plataforma Sul Americana com base na geoquímica Sm–Nd. Unpublished Doctoral Thesis. Universidade de São Paulo, Brazil, 301 pp.

Sato, K., Siga Jr., O., 2002. Rapid growth of continental crust between 2.2 to 1.8 Ga in the South American Platform: integrated Australian, European, North American and SW USA crustal evolution study. Gondwana Res. 5, 165–173.

Scarrow, J.H., Ayala, C., Kimbell, F.S., 2002. Insights into orogenesis: getting to the root of a continent–ocean–continent collision, Southern Urals, Russia. J. Geol. Soc. Lond. 159, 659–671.

Solar, G.S., Pressley, R.A., Brown, M., Tucker, R.D., 1998. Granite ascent in convergent orogenic belts: testing a model. Geology 26, 711–714.

Stacey, J.S., Kramers, J.D., 1975. Approximation of terrestrial lead isotope evolution by a two-stage model. Earth Planet. Sci. Lett. 26, 207–221.

Torquato, J.R., Cordani, U.G., 1981. Brazil–Africa geological links. Earth Sci. Rev. 17, 155–176.

Truckenbrodt, W., Góes, A.M., Nascimento, M.S., 2003. Minerais pesados em depósitos fanerozóicos no nordeste do Pará e noroeste do Maranhão. In: 8th Simpósio de Geologia da Amazônia, Resumos Expandidos (CD-ROM).

Vanderhaeghe, O., Ledru, D., Thiéblemont, D., Egal, E., Cocherie, A., Tegyey, M., Milési, J.P., 1998. Contrasting mechanisms of crustal growth. Geodynamic evolution of the Paleoproterozoic granite-greenstone belts of French Guiana. Precambrian Res. 92, 165–193.

Villas, R.N.N., 1982. Geocronologia das intrusões ígneas na bacia do rio Guamá, nordeste do Estado do Pará. In: 2nd Simpósio de Geologia da Amazônia, Anals, vol. 1, pp. 233–247.

Villas, R.N.N., 2001. O granito de duas micas Ney Peixoto, nordeste do Estado do Pará: caracterização petrográfico-petroquímica e contexto tectônico. In: 7th Simpósio de Geologia da Amazônia, Resumos Expandidos (CD-ROM).

Wanderley Filho, J.R., 1980. Geocronologia do Granito Mirasselvas, nordeste do Pará. Congresso Brasileiro de Geologia, 31, Camboriú, vol. 2, p. 426 (Abstracts).

Windley, B., 1992. Proterozoic collisional and accretionary orogens. In: Condie, K.C. (Ed.), Proterozoic Crustal Evolution. Elsevier, Amsterdam, pp. 419–446.